Acta Zoologica

Published for the Royal Swedish Academy of Sciences and the Danish Academy of Sciences and Letters

Acta Zoologica (Stockholm) **98**: 191–213 (April 2017) doi: 10.1111/azo.12164

The cnidome and internal morphology of *Lophelia pertusa* (Linnaeus, 1758) (Cnidaria, Anthozoa)

Susanna M. Strömberg[1] and Carina Östman[2]

[1]Dept. of Marine Sciences, University of Gothenburg, SE-452 96 Strömstad, Sweden; [2]Evolutionary Biology Centre, Uppsala University, Norbyvägen 18 A, SE-752 36 Uppsala, Sweden

Keywords:
Lophohelia prolifera, morphology, histology, cnidocyst, cnidoblast

Accepted for publication:
1 March 2016

Abstract

Strömberg, S.M., Östman, C. 2017. The cnidome and internal morphology of *Lophelia pertusa* (Linnaeus, 1758) (Cnidaria, Anthozoa). – *Acta Zoologica* (Stockholm) **98**: 191–213.

The cnidome of the scleractinian cold-water coral *Lophelia pertusa* (Linnaeus, 1758, syn. *Lophohelia prolifera*) was described by Carlgren in 1940. Due to a renewed interest in the cnidae of *L. pertusa,* specifically comparisons of adult and larval cnidae and their functions, we now redescribe the cnidome from material collected at the Tisler reef in Norway, close to Carlgren's collection site at Saekken (Sweden). Cnidae from column, tentacles, actinopharynx, mesenterial filaments and acontia were investigated. Fresh tissue preparations were compared to histological preparations of decalcified polyps to verify the presence of cnidocysts and secretory cells, and their composition and organization within tissues. The cnidome included microbasic b-mastigophores, microbasic and mesobasic p-mastigophores, holotrichous isorhizas and spirocysts. The nematocyst type cnidae (b-, p-mastigophores, isorhizas) appeared in different size classes with different distributions within the tissue. Spirocysts were highly variable in shape and size, without distinct size classes. In addition, developing stages of cnidae were documented, with new observations on the succession of p-mastigophore shaft development. The present observations were in general congruent with the cnidocyst descriptions from *L. prolifera* made by Carlgren; however, a tiny cnida, possibly of isorhiza type, has been added. Finally, the use of the term acontia is discussed.

Susanna M Strömberg, Dept. of Marine Sciences, University of Gothenburg. SE-452 96 Strömstad, Sweden. E-mail: susanna.stromberg@marine.gu.se

Introduction

Lophelia pertusa (Linneaus, 1758) is the most common reef-building cold-water coral with a nearly global distribution, ranging from Barents Sea to New Zealand. The depth range spans from 39 m in the Trondheim Fjord in Norway to 3383 m at the New England Seamount chain in the North Atlantic Ocean (Freiwald *et al.* 2004). The colonies have a branching growth pattern (Fig. 1A), with individual corallites of c. 10 mm diameter, and c. 20 mm in length (Gass and Roberts 2010). The vegetal growth consists of the budding of new individual polyps from the rim of the corallite of older polyps (Fig. 1B). Approximately the outermost 1 m layer of corallites contain live polyps, while older polyps beneath die due to reduced water exchange and food supply (Wilson 1979). The dead coral branches soon become colonized with a wide range of associated fauna, while the live parts of the colonies tend to be devoid of epifauna.

Deep-sea corals such as *L. pertusa* are azooxanthellate, that is lacking symbiotic photosynthesizing dinoflagellates. Studies have shown *L. pertusa* to be opportunistic feeders, utilizing both dissolved and particulate organic matter, picoplankton (e.g. bacteria) and zooplankton (Dodds *et al.* 2009; Mueller *et al.* 2013). In the North Sea, the relatively large (2–4 mm) copepod *Calanus finmarhicus* is common and shown to be included in the diet of *L. pertusa* (Dodds *et al.* 2009). With such large prey, one could suspect that *L. pertusa* would invest in heavy cnidocyst armament.

Cnidocysts function in food capture, defence, aggression and locomotion and can be divided into three functional types: (i) penetrating (toxin delivering), (ii) ensnaring (or volvent) and (iii) glutinant cnidae (Mariscal 1984; Colin and

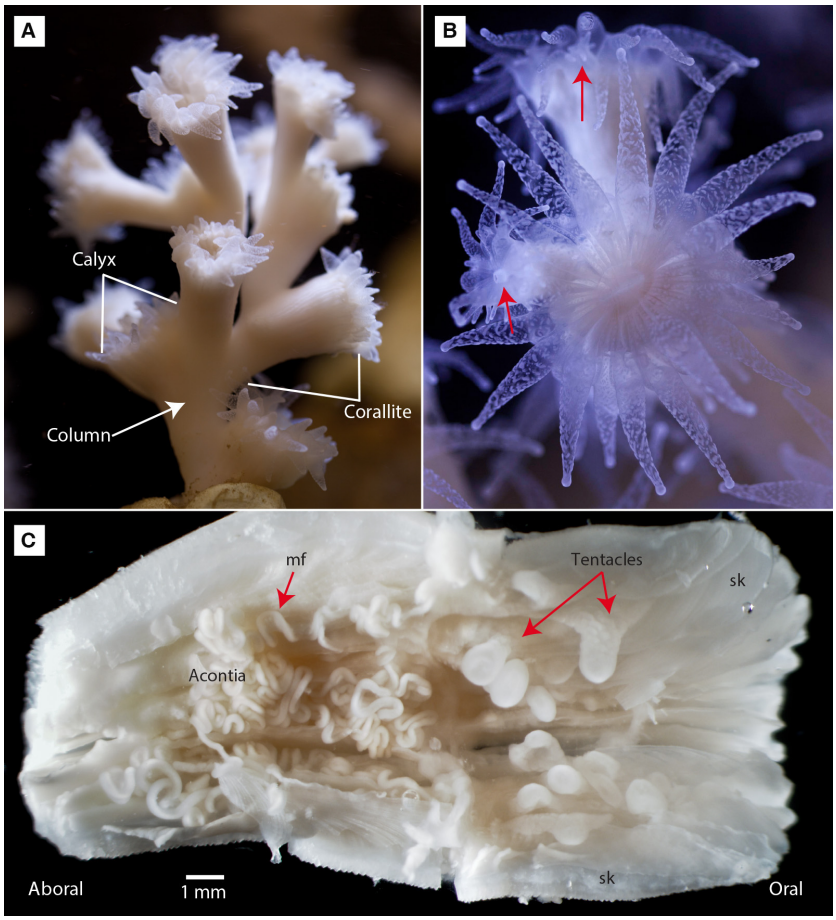

Fig. 1—General anatomy of *Lophelia pertusa*. – A. Colony morphology (tentacles semi-retracted). – B. Fully extended tentacles showing white blotches of cnidocyst batteries and the oral disk with mouth/actinopharynx in the centre. Red arrows point out young buds; on the lower, the actinopharynx is visible as a cylinder. – C. A corallite cut longitudinally: retracted tentacles at oral end, acontia at aboral end, mesenterial filaments (mf) attached via the mesenteries to the walls and part of the oral disk ripped apart in the middle. Skeletal lamellae/septa (sk). Corallites c. 10 mm in diameter.

Costello 2007). Glutinant cnidae are the most versatile and can function both in prey capture, tube building and in locomotion (Kass-Simon and Scappaticci 2002). Cnidocysts are classified into three categories based on morphological characters: nematocysts, spirocysts and ptychocysts. Nematocysts include penetrating and ensnaring cnidae. The other two categories are glutinant (Mariscal *et al.* 1977a,b). The highest diversity is found among nematocysts within Hydrozoa. In Anthozoa, a mere 10 of the total 30 types are present; instead, the anthozoans have added spirocysts and ptychocysts (Fautin and Mariscal 1991; Östman 2000; Kass-Simon and Scappaticci 2002; Fautin 2009).

Once a cnida is fired, it is wasted, and there is a constant replenishing of armament. Cnidogenesis has been described by Slautterback and Fawcett (1959), Skaer and Picken (1966), Westfall (1966), Skaer (1973), Holstein (1981), Tardent and Holstein (1982), among others, reviewed by Kass-Simon and Scappaticci (2002). Documentation of the morphology of developing cnidae (cnidoblasts) in different stages of maturation has been carried out for the anthozoans *Metridium senile* and *Sagartiogeton viduatus* by Östman *et al.* (2010a, b, 2013). Möbius (1866) suggested that cnidoblasts differentiate beneath the mature cnidocytes (commented in Robson 2004). Slautterback and Fawcett (1959) traced the origin of cnidoblasts from interstitial cells at the base of the epithelium. The maturing cnidae are subsequently migrating from the basal to the distal epithelium where the final maturation takes place (Skaer 1973; Tardent 1995).

The cnidome of *Lophohelia prolifera* was described by Carlgren in 1940 from material collected at Saekken in the Koster Trough (Bohuslän, Sweden, aprox. 59°00.82′N, 11°06.96′E). He also included samples from the Drontheim Fjord (i.e. Trondheim Fjord, Norway). Carlgren separated the soft tissues from column, tentacles, actinopharynx and filaments (i.e. mesenterial filaments and acontia), and recorded cnidae type composition and size classes in the different tissues (Table 1).

The name *Lophohelia prolifera* is a homonym including *Lophelia pertusa*, *Madrepora oculata* and *Solenosmilia variabilis* (Fautin 2013). Later studies have confirmed the only species present at the sampling site of Carlgren to be *L. pertusa* (e.g. Dahl *et al.* 2012), and further studies on reproduction, embryology and larval development of *L. pertusa* from the area led to a renewed interest in the cnidome.

Larsson *et al.* (2014) observed cnidocyst discharge in planulae from 30 days of age and onwards, coinciding with

Table 1 Cnidome of *Lophohelia prolifera* (syn. *Lophelia pertusa*), from Carlgren (1940, pp 44–46). Length-to-width ranges of capsules (in μm)

Tissue and cnidae type	Length × width (μm)	Carlgren's remarks
Column		
p-mastigophores	17–20 × 5.5	'very numerous'
Tentacles		
b-mastigophores	32.5–42.5 × 4–5	'fairly sparse, shaft very short, 3 spine rows'
p-mastigophores	18 × 5.5	
p-mastigophores	36–46 × 5	'common, hoplotelic[2], everted shaft of capsule length, 10 spine rows'
holotrichs[1]	49–55 × 14–17	'sparse'
spirocysts	–	'very numerous'
Actinopharynx		
b-mastigophores	22–34 × 4–4.5	'sparse, like those of the tentacles'
p-mastigophores	14–17 × 5	'sparse, more or less oviform'
holotrichs[1]	60 × 12–14	'rare'
Filaments		
b-mastigophores	14–22.5 × 3	'sparse'
p-mastigophores	23–46 × 6–8	'possibly not hoplotelic[2], numerous'
p-mastigophores	73–101 × 11–13	'hoplotelic[2], only in the lower, strongly coiled parts of the filaments [i.e. acontia], sparse, 15 spine rows'
holotrichs[1]	79–94 × 13–16	'very closely situated, only in the lower, strongly coiled parts of the filaments' [i.e. acontia]
spirocysts	–	'very rare, seem to occur also in the mesenteries'

[1]holotrich = tubule spined throughout, corresponds to isorhizas.
[2]hoplotelic = shaft and distal tubule spined.

the onset of bottom-probing behaviour. The actinula larva of the hydrozoan *Tubularia mesembryanthemum*, Allman 1871 (accepted as *Ectopleura crocea* [Agassiz, 1862], WoRMS Editorial Board 2014) has been shown to use atrichous isorhizas for primary anchoring during settling (Yamashita *et al.* 2003). It was therefore hypothesized that the presence of cnidocysts in *L. pertusa* planulae is an indication of competence to settle and thus an interesting aspect of larval development. To be able to pinpoint the onset of settling competency is a valuable piece of information when constructing larval dispersal models, and the main incentive for conducting these studies.

The aim of this study was to redescribe the cnidome of adult polyps of *L. pertusa* to be able to compare cnidae of adults and planulae, with the purpose of investigating differences in adult and larval cnidae form and function.

Materials and Methods

Lophelia pertusa were collected by an ROV (Remotely Operated Vehicle) from the Tisler reef in northeast Skagerrak, Norway, on 21 December 2012 (87–105 m depth at positions between 58°59′41.4″N, 10°58′07.4″E and 58°59′39.5″N, 10°58′06.4″E). The collected specimens were brought to the field station of the University of Gothenburg at Tjärnö (58°52′33.92″N, 11°8′46.60″E), situated on the west coast of Sweden and c. 10 nmi south of Tisler and Saekken. The corals were kept in flow-through aquaria with filtered seawater (5 μm Ametek polypropylene cartridges). Water temperature and salinity were kept close to *in situ* values (7–8 °C, 34–35 psu) in a constant temperature room. The corals were fed with homogenized *Calanus* copepods twice a week. The sampled corals were also used in reproductive and larval studies, and rearing methods are further described in Larsson *et al.* (2014).

Cnidocyst sizes and cnidae type composition in different tissues from newly collected *L. pertusa* were compared to the cnidocyst descriptions made by Carlgren (1940) from *Lophohelia prolifera*. In addition, preparations of live tissues of *L. pertusa* were compared to haematoxylin and eosin-stained sections of histological preparations of decalcified polyps to verify the presence of cnidocysts and secretory cells (unicellular glands), and their composition and organization within tissues.

Fresh tissue preparation

Dissections were carried out by first cutting the corallite (skeletal cup) longitudinally with a microtome knife (Fig. 1C), and then soft tissue was pinched out with a fine forceps, trying to get clean isolated tissue samples from the five discernible tissue types, that is tentacles, actinopharynx, mesenterial filaments and acontia. Live tissue from the column (outer wall of corallites) was scraped off with a scalpel and smeared on a glass slide. Care was taken to avoid

cross-contamination of cnidocysts between tissue types; however, some cnidae were probably displaced.

The tissues were observed under an Olympus BX51 light microscope equipped with an Olympus DP70 camera, both as wet preparations of tissues with intact integrity immediately after dissection and as squash preparations, semi-dry to dry after a few hours. Usually, the cover slip was allowed to gently squash the tissues as the sample dried, rather than squashing by force. Some tissue slides were stained with a nigrosin and eosin mix (Hancock Stain). Nigrosin gives a background coloration to visualize transparent cells, as the cell membranes repel the negatively charged carbon particles and remain clear against the purplish black background. It was especially suitable for visualizing the everted shaft and tubule of nematocysts. Eosin stained some components of the spirocyst tubule well, even when still within the capsule. The developing stages of spirocysts stained with both nigrosin and eosin and were very well visualized with this method. Other cnidae types did not stain with eosin in fresh preparations.

Histological preparation

Coral samples were fixed in a modified Helly's solution (containing zinc chloride and potassium dichromate, $K_2Cr_2O_7$), and postfixed with a 3% aqueous solution of potassium dichromate, washed in several water baths, decalcified with formic acid and stored in 50% or 70% ethanol, before and/or after decalcification. The polyps were embedded in paraffin with a melting point of 55–58 °C and cut into 4 or 6 μm sections. Staining of sections was carried out with Harris's haematoxylin and eosin, sometimes with glacial acetic acid added to the eosin. The acid reduced the intensity of haematoxylin and gave more nuance and detail to some aspects of the morphology. Xylene was used for deparaffinization and clearing. The slides were finally mounted with Pertex and observed and photo documented under light microscopy (as described above).

Measurements

Cnidocyst measurements were made from photomicrographs with the image analysis software Image J (version 1.45s, Abramoff *et al.* 2004). A test of the accuracy was made by measuring cnidae of different size classes with 6 replicate measurements each. Measurements had a standard deviation with a range of ±0.1–0.3. Cnidocysts with sufficient detail were measured, and the number of measured cnidae somewhat reflects the abundance of each type, in each tissue. Smaller cnidae were, however, probably underestimated due to difficulties of observation. Likewise, very abundant cnidae types were left unmeasured when sufficient numbers were achieved. A total of 1376 cnidocysts were measured, from 7 different polyps, although not all tissues were covered in each polyp. The individual variation between polyps can therefore not be deduced from the present data. Whether cnidae types were divided into distinct size classes was investigated in a series of histograms on size frequency distributions presented in Fig. 2A–F and supplemental material (S1, Supplemental tables and graphs).

Nomenclature

Cnidae were identified by size, shape and morphology of their undischarged and discharged capsule, shaft and tubule, including spine armature. The classification system and nomenclature of cnidocysts, including nematocysts and spirocysts, established by Weill (1934) with modifications made by Carlgren (1940), Cutress (1955), Mariscal (1974), Östman (2000) and Östman *et al.* (2010a) were used.

Throughout this study, we will use *cnidocysts* as the common denotation for all cnidae types, while *nematocysts* will refer to isorhizas, p-mastigophores and b-mastigophores, thus excluding spirocysts. The cnido*cysts* are the organelles (capsule and content). The cnido*blasts* are the cells housing the developing cnido*cysts*, while the cells containing the mature cnidocysts are called cnido*cytes*. The suffixes *-blast*, *-cytes* and *-cysts* will sometimes be added to the roots *nemato-* or *spiro-* when specific types are discussed.

The proper recognition of different types of secretory cells is beyond the scope of this paper. A distinction can be made between basophilic mucocytes and acidophilic granular gland cells; however, beyond this, the cellular detail in this study does not allow further distinction.

Finally, we have chosen to use the term acontia for the free coils of the mesenterial filaments. This term has previously not been used in scleractinian morphology; we therefore provide a justification for this in the discussion.

Results

Tissue morphology and organization

Column. The thin tissue layer of the thecal wall (referred to as the column by Carlgren 1940) contained surprisingly

Fig. 2—Frequency distributions of cnidae sizes and their distribution over tissues. – A–B. Size distributions of b- and p-mastigophores in all tissues with size spans marked out for the separate tissues with color-coded lines. – A. The b-mastigophores are divided into two main size classes: small (12–22 μm) and large (30–48 μm), with a few intermediate (23–29 μm). – B. The p-mastigophores could be divided into four size classes: small (13–22 μm), medium (23–34 μm), large (35–69 μm) and very large (70–138 μm). Dotted part of the line for acontia p-mastigophores denotes low abundances. Trend lines in A–B are based on two point moving averages. C–D. Size distributions of isorhizas in acontia (C) and tentacles (D). Sizes were non-overlapping in the different tissues, with isorhizas in tentacles approx. half the length compared to acontia isorhizas. – E–F. Size distributions of spirocysts in tentacles (E) and actinopharynx (F) with overlapping size range.

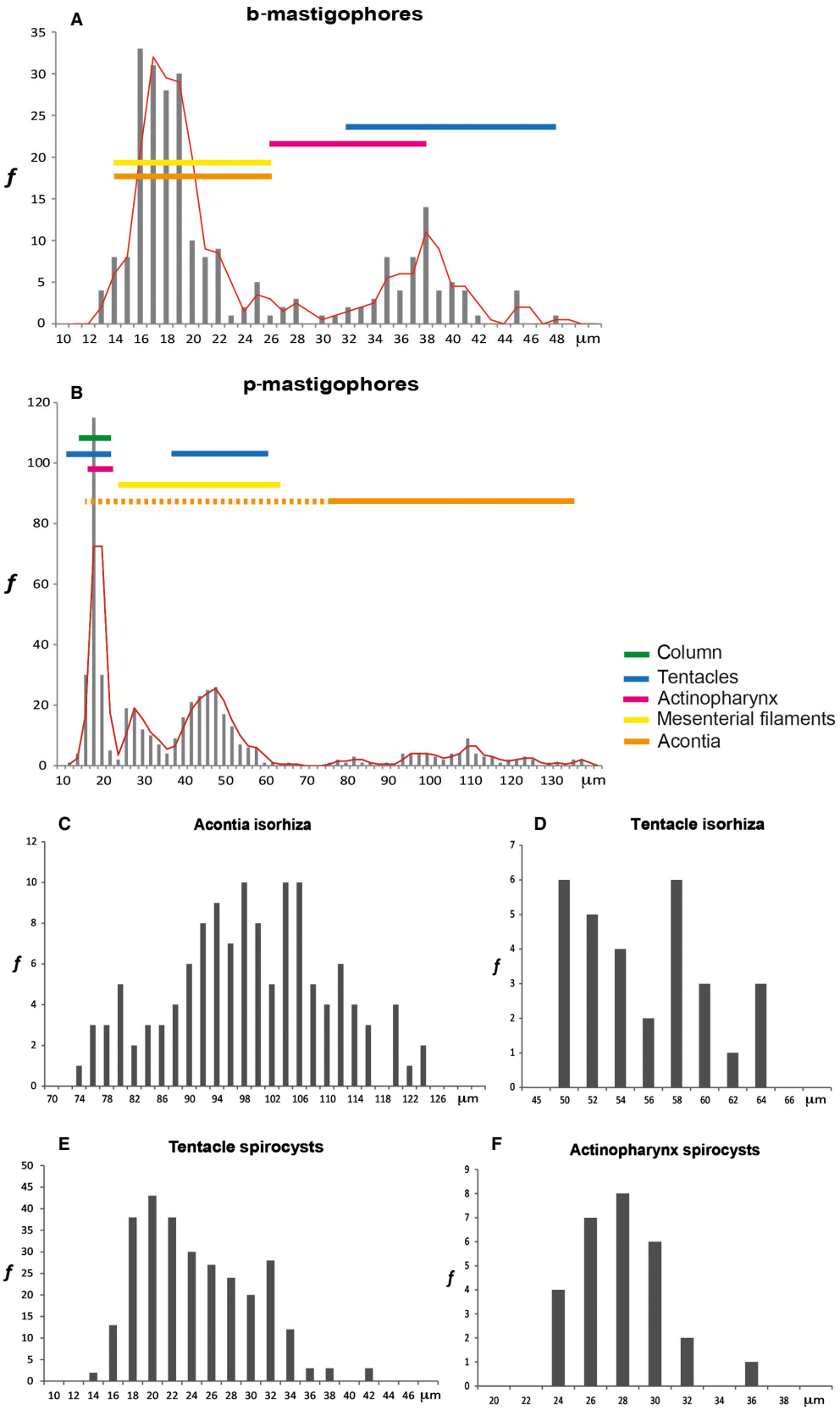

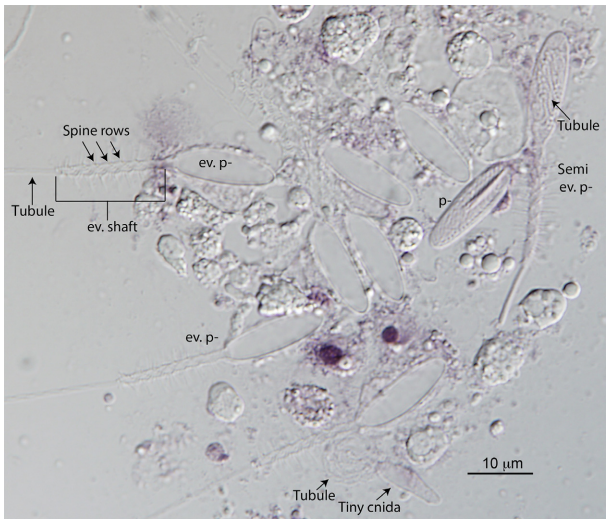

Fig. 3—Live tissue smear from corallite/theca wall (column). Small p-mastigophores: intact (p-); semi-everted (semi ev. p-) with everted shaft but tubule still in capsule; and fully everted (ev. p-). A tiny cnida (isorhiza) with its everted coiled tubule [Colour figure can be viewed at wileyonlinelibrary.com].

abundant numbers of nematocysts, dominated by a homogenous population of small microbasic p-mastigophores with rounded oval capsules (Fig. 3, Tables 2 and 3, S2 p.3). A few tiny (range: 7–9 μm) cnidae, probably of isorhiza type, were observed interspersed among the small p-mastigophores.

Tentacles. On live polyps with extended tentacles, the tentacle surface was spattered with irregular whitish blotches of reflective cnidocyst batteries, with translucent tissue in between (Fig. 1B). The terminal knobs (acrospheres) at the tentacle tips were uniformly whitish, capped with cnidocysts and with a slight constriction at the base of the knob. At the very apex of the tentacle tip a hydro pore (or terminal pore) was observed, visible with light microscopy in intact, fresh preparations of tentacles (Fig. 4A). The cnidocysts were oriented with their apical ends towards the pore. Dense aggregates of mucocytes were observed in the epidermis between cnidocyst batteries on the surfaces of the contracted tentacles (Fig. 4B–C).

All cnidae types were present in the tentacles (Tables 2, 3). Spirocysts dominated overall, while microbasic b- and p-mastigophores were numerous at the tip, and patchily dis-

Table 2 Cnidome of *Lophelia pertusa* (present study). Length-to-width ranges of capsules (in μm)

Tissue and cnidae type	Length × width (μm)	*n*	Remarks
Column – dominated by homogenous small p-mastigophores			
p-mastigophores, small	13.9–20.8 × 3.8–6.2	111	Numerous
tiny cnidae	7.0–9.4 × 1.9–2.7	13	Sparse
Tentacles – dominated by spirocysts, all types present, rich in mucocytes			
b-mastigophores, large	31.4–47.6 × 4.0–6.0	50	Common, patchy, shaft with 4–5 spine rows
p-mastigophores, small-(medium)[1]	13.6–27.0 × 2.9–7.6	49	Common, patchy, shaft with 7-9 spine rows
p-mastigophores, large	35.2–58.3 × 5.0–9.6	102	Numerous, patchy, 15 and 18 spine rows
isorhizas, broad oval	45.6–63.0 × 13.9–23.1	30	Sparse
tiny cnidae	8.2–11.3 × 1.8–3.1	18	Sparse
spirocysts	12.3–41.7 × 1.7–7.2	284	Very numerous
Actinopharynx – oral disc epidermis dominated by mucocytes, actinopharynx epidermis ciliated and rich in secretory cells			
b-mastigophores, medium-large	24.4–37.9 × 2.8–5.1	19	Sparse
p-mastigophores, (small)[1]-medium	15.9–37.5 × 5.0–8.0	23	Sparse
spirocysts	23.7–34.7 × 1.0–7.0	28	Sparse
Mesenterial filament – secretory cells and medium p-mastigophores dominated			
b-mastigophores, small-(medium)[1]	12.3–24.1 × 2.3–5.1	108	Numerous, shaft with 3 spine rows
p-mastigophores, (small)[1]-medium	16.0–34.4 × 3.1–11.0	118	Numerous, shaft with 12 and 15 spine rows
p-mastigophores, large	35.2–63.4 × 4.9–13.3	105	Numerous, shaft with 18 and 20 spine rows
isorhizas, broad oval + large narrow	45.0–87.2 × 5.1–18.3	9	Contamination from acontia and tentacles? Not confirmed from histology
tiny cnidae	6.4–9.2 × 2.2–2.7	4	Rare
spirocysts	21.9–48.0 × 3.4–6.4	13	Contamination from tentacles? Not confirmed from histology
Acontia – dominated by large narrow isorhizas and very large p-mastigophores			
b-mastigophores, small-(medium)[1]	12.9–25.1 × 2.3–5.2	67	Shaft with 3 spine rows
p-mastigophores, small-large	13.9–64.8 × 4.2–13.6	22	Sparse
p-mastigophores, very large	74.7–137.7 × 9.8–16.9	75	Numerous, shaft with 28 or 38 spine rows
isorhizas, large narrow	73.4–123.9 × 14.0–21.8	126	Numerous
tiny cnidae	6.4–8.3 × 1.4–2.7 2	Rare	
		1376	N

[1]Minor contribution of size class in brackets, see Table 3.

Table 3 *Lophelia pertusa:* cnidae type and size class distribution over tissues with ranked abundances ([1])

Cnidae type	Size class	Range (μm)	Column *n*	Tentacles *n*	Actinoph *n*	Mesfil *n*	Acontia *n*
b-mast	Small	12–22				111[4]	67[3]
	Medium	23–29			8[1]	2[1]	2[1]
	Large	30–48		50[3]	11[2]		
p-mast	Small	13–22	111[4]	47[3]	5[1]	5[1]	3[1]
	Medium	23–34		3[1]	18[2]	113[4]	7[1]
	Large	35–69		102[4]		105[4]	12[2]
	Very large	70–138					75[4]
isorhiza	Large	46–63		30[2]		8[1]	
	Very large	73–124			1[1]		128[5]
tiny		6–11	13[2]	17[2]	4[1]		2[1]
spirocysts		z12–42	284[5]	28[2]	13[2]		

[1]Rare.
[2]Sparse.
[3]Common.
[4]Numerous.
[5]Very numerous.

tributed along the tentacles. The microbasic b-mastigophores found in the tentacles were larger than those found in other tissues (Fig. 2A, 4E). The p-mastigophores were found in two discrete size classes, small and large (Figs 2B, 4D–E), with a few medium sized (n = 3) included in the small category. Tiny cnidae of isorhiza type were also observed in the tentacle tissue, similar to those found in the column, with a spiraled or bent everted tubule. A few broad oval isorhizas were observed scattered among the other cnidocysts (Figs 2D, 4F). The spirocysts were highly variable in size (Figs 2E, 4D–F).

In histological preparations, the distal and basal epidermis, the mesoglea bordered by muscle fibres, the gastrodermis and tentacle lumen (i.e. endo-/exocoel) were clearly distinguishable (Fig. 5A–C). Cross sections at the base of the tentacles were oval, while sections through more apical parts were circular (Fig. 5B). The distal part of the epidermis was stained intensely pink and blue by abundant cnidocysts and mucocytes. The basal part of the epidermis was unusually wide in some tentacle cross sections. It was rich in nuclei and contained a frilly matrix of fibres, that is extensions of the myonemes from epitheliomuscular cells lining the mesoglea, and possibly components of the subepidermal nerve net. Cnidoblasts were found in the basal epidermis, close to the mesoglea (Fig. 5A, C).

Spirocysts were the most conspicuous cnidae type, while other types were less well visualized with the methods used. The spirocysts were found in bundles embedded between mucocytes, oriented with their broad apical tubule coil and capsule end towards the surface and their narrow end rooted in the epidermis (Fig. 5A–C). Their stark pink-stained coils of tubule easily identified them in the tissue. In cross-sectioned acontia, the spirocyst tubules were visible as red circles (Fig. 5A, right end). Possible p- or b-mastigophores were sometimes seen as pale pink fusiform structures, surrounded by a pink haze, that is the shaft and tubule, respectively (Fig. 5C). The few holotrichous isorhizas observed in histological preparations of tentacles were occasionally embedded deeper in the epidermis than the other cnidae (S2 p.4) and could be identified by their larger size and more diffuse and oblique undulating coils.

Actinopharynx. In live corals, the actinopharynx is seen as a compressed cylinder in the middle of the oral disc, connecting the gastrovascular cavity to the outside (Figs 1B, 6A). The opening is surrounded by a protruding rim (similar to lips), that is the peristome. When the polyp opens the mouth the partition walls of the endo- and exocoelic compartments under the oral disc can be seen as white stripes in the opening (Fig. 6A). During dissections, this was also the character used for detecting the actinopharynx. When the stripes were observed, the tissue around them was pinched out with fine forceps.

The oral disc epidermis was dominated by mucocytes, sparingly interspersed with spirocysts (seen in histological sections). In fresh preparations, medium to large b-mastigophores (Figs 2A, 6C) and small oval p-mastigophores (Figs 2B, 6B) were present, but could not be confirmed on histological slides. In sections cut through the oral disc, lateral and parallel to the oral aperture, the endo- and exocoelic compartments under the oral disc were visible (Fig. 6D–D′). Large bundles of muscle fibres were observed lateral to the actinopharynx (Fig. 6E–E′). The epidermis of the actinopharynx was densely ciliated (Fig. 6F–F′) and stained heavily from haematoxylin, rich in gland cells and possibly other basophilic components. Overall, the epidermis of the oral disc and the actinopharynx seems the least cnidocyst laden of all tissues (Tables 2, 3).

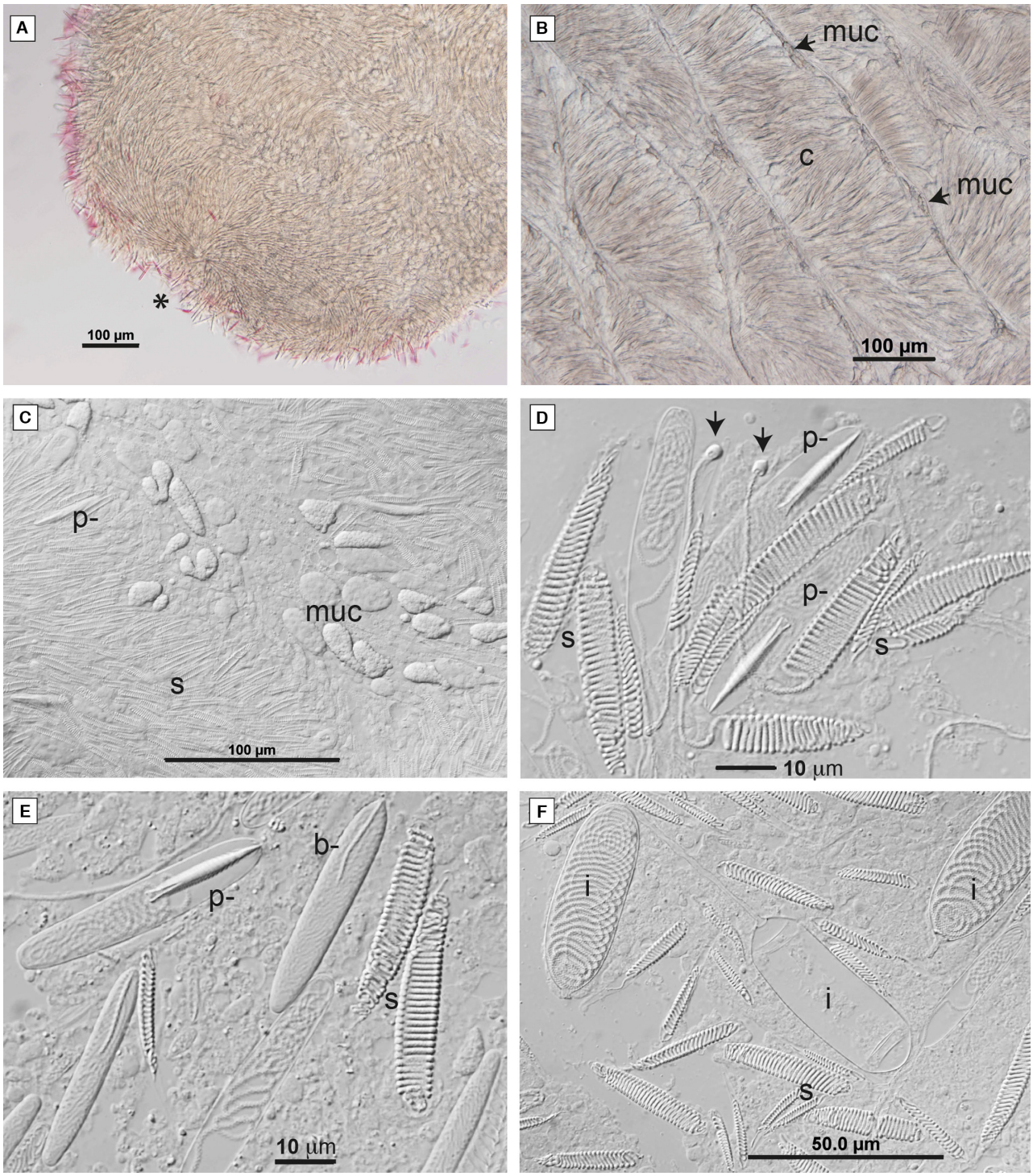

Fig. 4—Fresh preparations of tentacles. – A. Tentacle tip (acrosphere) with visible terminal pore (*). Cnidae are oriented with their apical ends towards the pore. Some spirocysts are stained pink from eosin. – B. Close-up of contracted tentacle: cnidocyst batteries (c) with mucocytes (muc) in between. – C. Tentacle surface at higher magnification with spirocysts (s), p-mastigophore (p-) and mucocytes (muc). – D-F. Close-ups of tentacle cnidae. – D. Spirocysts (s) and p-mastigophores (p-). Distal ends of semi-everted tubules of spirocysts capped with agglutinant liquid (arrows). – E. Spirocysts (s), p-mastigophore (p-) and b-mastigophores (b-). – F. Spirocysts (s) and broad oval isorhizas (i), the latter both everted and intact [Colour figure can be viewed at wileyonlinelibrary.com].

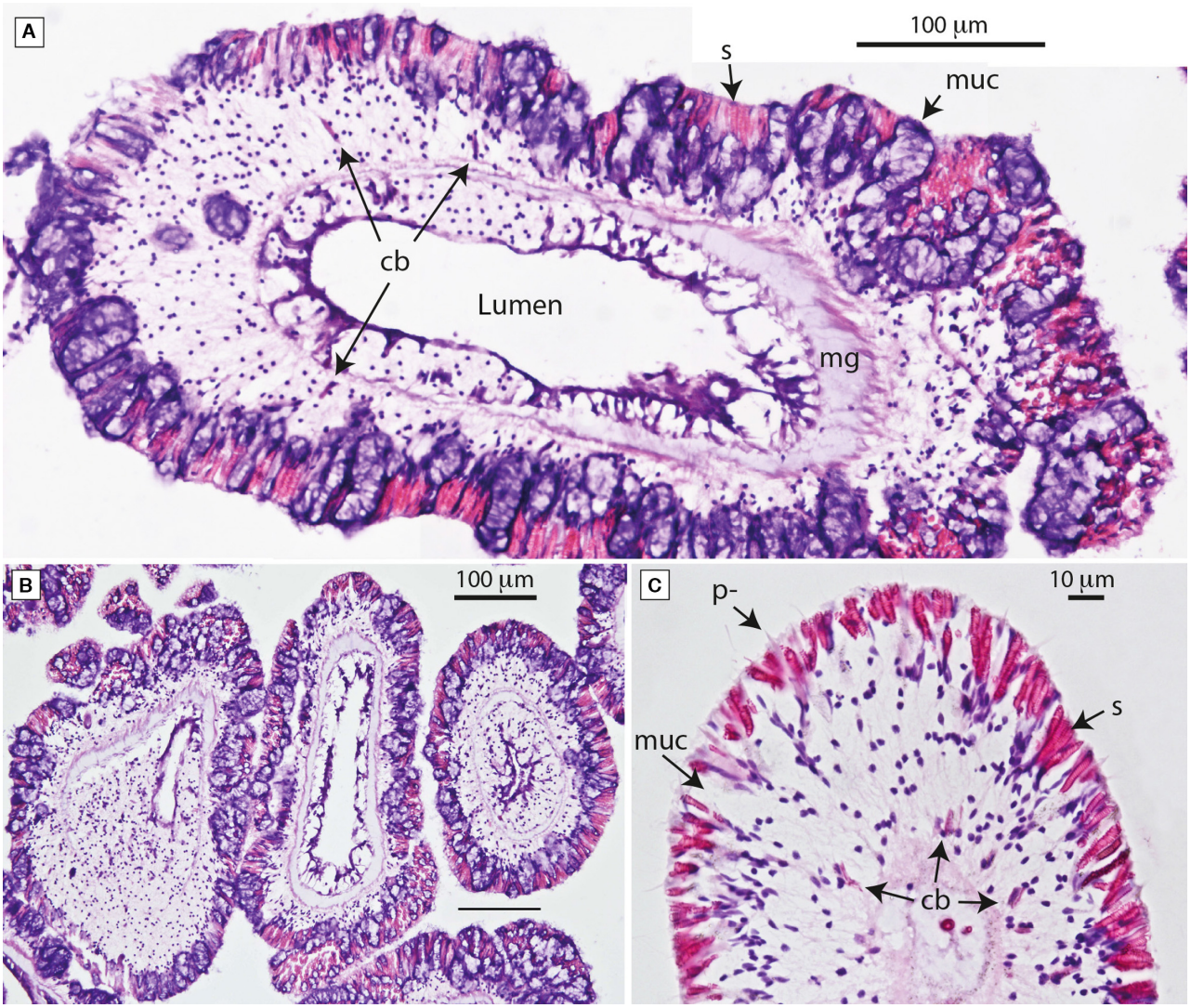

Fig. 5—Histological preparations of tentacles. – A. Cross section of tentacle, cut slightly oblique at the base. Epidermis facing outwards: distal part contains spirocysts (s) and mucocytes (muc); basal epidermis contains nuclei (dark dots) and a frilly matrix (pink fibres), possibly myonemes, that is extensions of the epitheliomuscular cells lining the mesoglea (mg). Arrows point out cnidoblasts (cb). The gastrodermis faces the lumen (left side intact, gastrodermal cells damaged on the right side). The tentacle lumen is continuous with the endo-/exocoels. – B. Cross sections of three tentacles. – C. Part of a cross-sectioned tentacle close to the tip (lumen not present). Acid was added to the eosin, and hematoxylin stain was partially lost; mucocytes (muc) are therefore seen as empty voids. Spirocysts (s) with dark pink-stained coils, possible pmastigophores (p-) seen as lighter pink fusiform shapes. Arrows point out cnidoblasts (cb).

Mesenterial filaments. In fresh squash preparations, the mesenteries were seen as muscular membranes with an undulating swollen edge, that is the cnidoglandular band (CGB, Fig. 7A–C). Adjacent to the CGB, the mesentery was thickened, and from their appearance in histological cross sections, this region has been named the *lateral lobes* (LL, Fig. 7E–F). Together, the CGB and lateral lobes constitute the mesenterial filament. The CGB were packed with cnidocysts, mucocytes and ciliated supporting cells (Fig. 7C–D). The lobes contained abundant secretory cells, and, if the animal had been fed recently, assimilated nutrients in the phagocytic or absorptive cells, such as lipid droplets and inclusions of carotenoids from the food (Fig. 7C). In both histological and fresh preparations, there was a distinct translucent band of tissue between the CGB and lobes, lacking any refractive components (Fig. 7A–C, E).

The CGB was dominated by microbasic p-mastigophores with a large variation in size and shape, some rounded oval (prolate spheroids) and some more diamond shaped (Fig. 7D). The size distribution was bimodal (Fig. 2B, S1

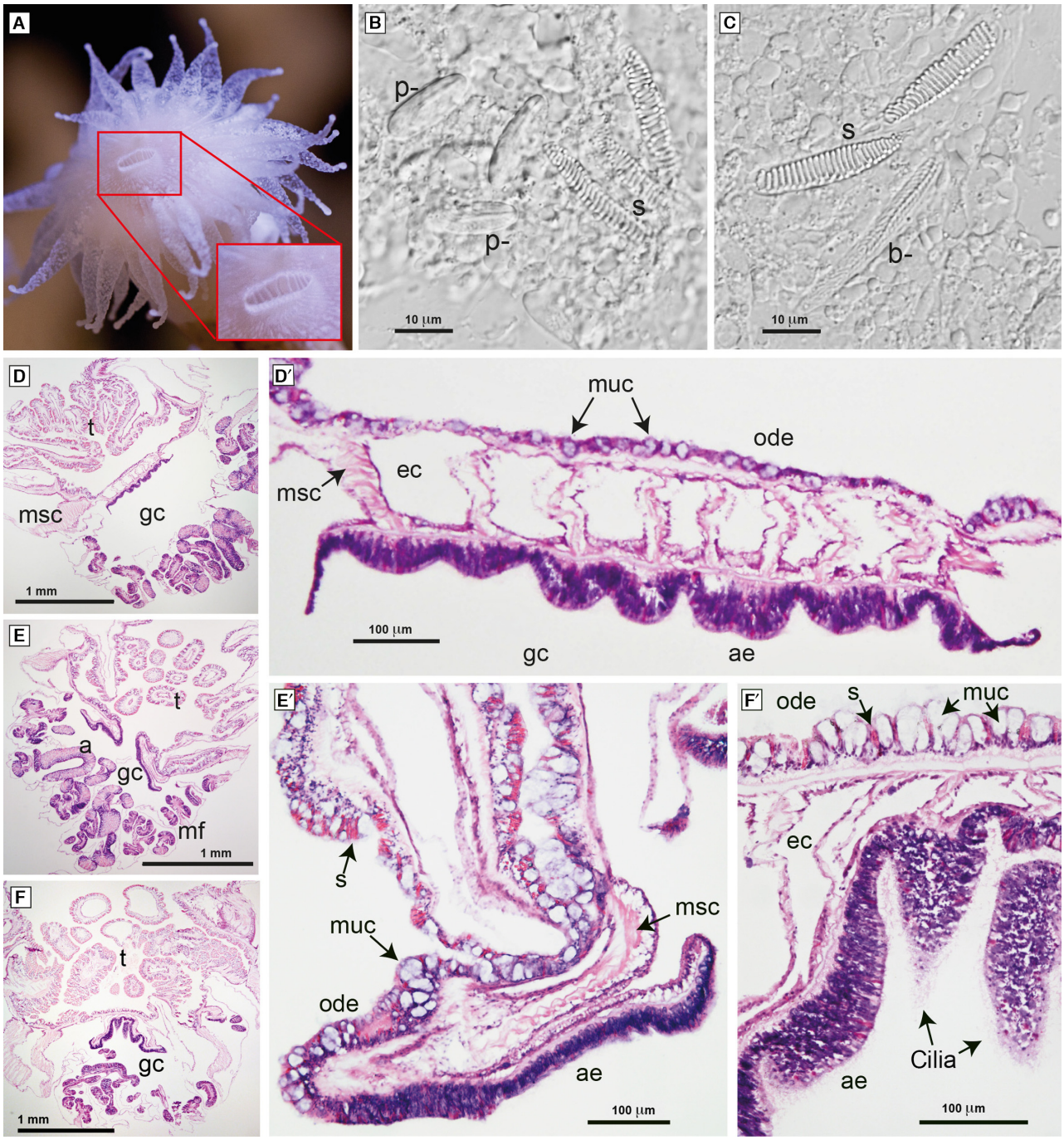

Fig. 6—Actinopharynx. – A. Polyp with open mouth: the white stripes are the partition walls of the body compartments (endo-/exocoels) under the oral disk, seen through the inner wall of the actinopharynx (inserted close-up). – B–C. Fresh tissue preparations from actinopharynx with small oval p-mastigophores (p-), spirocysts (s) and b-mastigophores (b-). – D, E, F. Whole-mounts of polyps with the actinopharynx centered and with corresponding close-ups in D′, E′ and F′. Gastrovascular cavity (gc) and tentacles (t) marked out for orientation. – D–D′. A parasagittal section of the actinopharynx, cut longitudinally adjacent to but not through, the opening. The body compartments, that is endo-/exocoels (ec), are visible between oral disk epidermis (ode) and actinopharynx epidermis (ae). Oral disk epidermis contains cnidocysts and mucocytes (muc), while the actinopharynx epidermis contains more basophilic components and is heavily ciliated. Muscle fibres (msc) in the mesenteries seen lateral to the actinopharynx. – E–E′. Actinopharynx cut through the oral pore. Acontia (a) and mesenterial filaments (mf). – F–F′. Actinopharynx cross-sectioned adjacent to the oral pore, with spirocysts (s), mucocytes (muc), endo-/exocoels (ec) and cilia visible in F′.

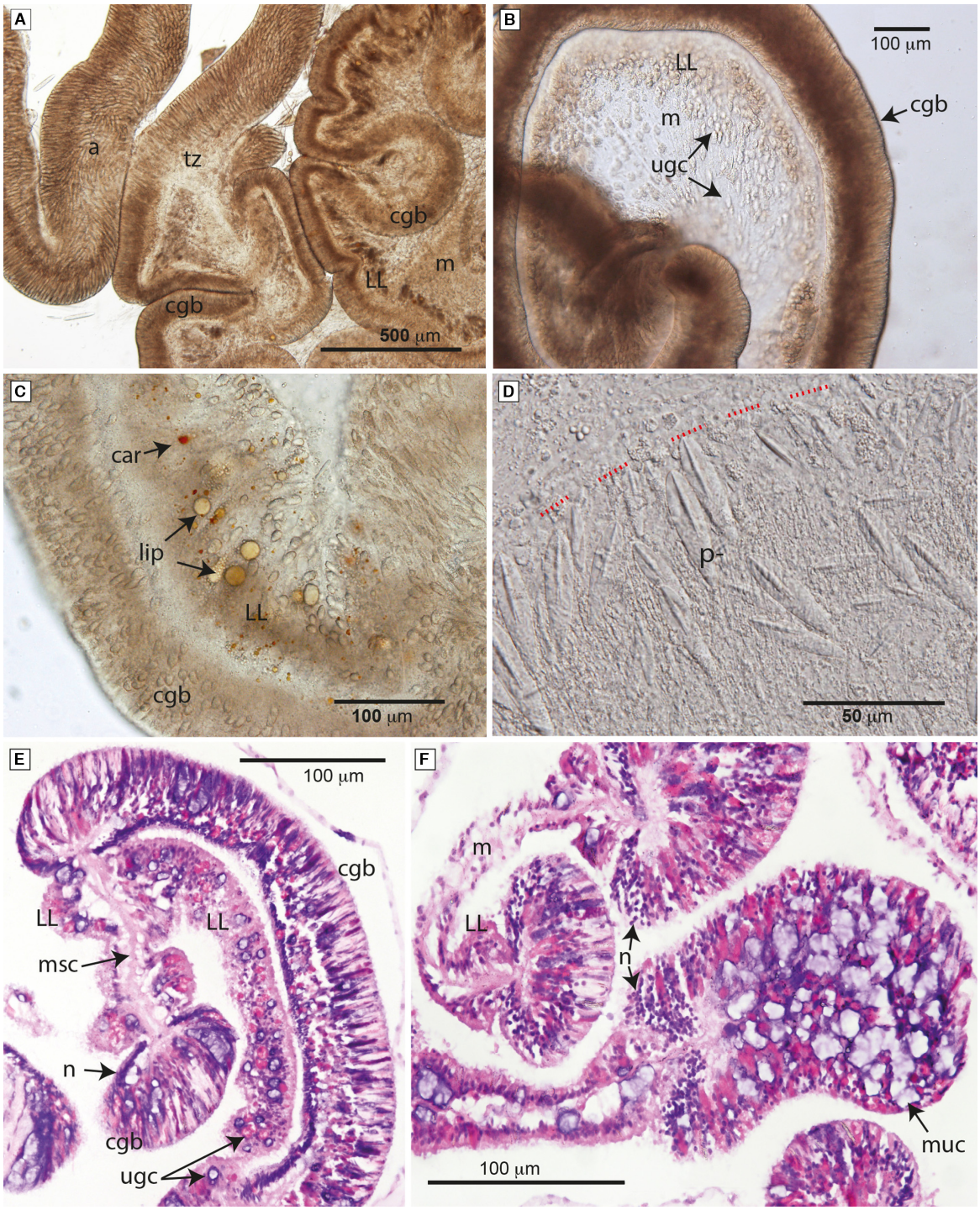

Fig. 7—Mesenterial filaments. – A. Transition zone (tz) between mesenterial filaments and acontia (a). The cnidoglandular band (cgb) and lateral lobes (LL) constitute the mesenterial filaments at the edge of the mesentery (m). – B. Part of mesentery (m) with cnidoglandular band (cgb) and lateral lobes (LL). Unicellular gland cells (ugc) are present throughout the mesentery, but appear denser in the lateral lobes (LL). – C. Stored nutrients in the lateral lobes (LL): lipid droplets (lip) and carotenoids (car). – D. Close-up of cnidoglandular band with diamond shaped p-mastigophores (p-); their apical ends with shafts towards the rim (red dotted lines). – E–F. Histological preparations of mesenterial filaments. – E. Longitudinal cut. Dense rows of nuclei (n) at the base of the cnidoglandular band (cgb) lateral to the attachments of muscle fibres (msc) from the mesentery. Lateral lobes (LL). Arrows also pointing out unicellular gland cells (ugc): mucocytes (blue) and acidophilic gland cells (pink). – F. Cross sections of cnidoglandular bands with large mucocytes (muc), nuclei (n), lateral lobes (LL) and part of mesentery (m) between.

p.12), including medium and large p-mastigophores (Tables 2, 3). Small b-mastigophores were abundant but inconspicuous. A few isorhizas and spirocysts were observed, although these were probably contaminations from other tissues, that is their presence could not be confirmed in histological sections.

In histological preparations, the mesenteries were heavily stained. Secretory cells were abundant, especially in the CGB and lobes (Fig. 7B, E–F). Unidentified dark purplish broad or elongate structures other than mucocytes were observed in the distal part of the gastrodermis in the CGB. Eosinophilic elongate structures were also observed, recognizable as p-mastigophores, while no spirocysts were observed (Fig. 7E–F). Also, in the lobes, pink blotches were observed, possibly acidophilic granular gland cells. Two dense lines of nuclei ran along the base of the CGB on each side of the muscle fibres from the mesentery anchored in between, with cnidocysts oriented in a fan-like manner from the base, with their apex towards the margin (Fig. 7E–F). Between the line of nuclei and the cnidocysts, pink and purple blotches were observed in the basal cell layer, probably cnidoblasts and gland cells. Even in lighter stained sections, the mesenterial filaments were too intensely stained to allow for reliable identification of all components, and thinner sections might have given better details.

Acontia. In fresh preparations, the acontia appeared as uniform long filaments densely packed with a distinct cnidae complement of very large nematocysts, different from the cnidae of the cnidoglandular band (CGB). Muscle fibres along the base mid-line allow them to contract in a spiral manner (Fig. 8A). Acontia emanated from the CGBs (along their lower parts), producing long free coils extending into the bottom of the gastrovascular cavity, and were of approximately twice the width compared to the CGB. Our examinations did not extend to investigating whether there were one or several acontia attached to each CGB. The transition zone between CGB and acontia was short and distinct (Fig. 7A).

Large and narrow holotrichous isorhizas dominated in the acontia, while very large p-mastigophores were patchily distributed, although sometimes abundant (Tables 2, 3, Fig. 8C). In between the very large nematocysts, small b-mastigophores and small p-mastigophores were observed. In squash preparations, medium and large p-mastigophores were also encountered, although not visible in intact acontia, and possibly associated with the transition zones, close to the CGB. A few cnidoblasts were observed among the densely packed nematocyst capsules (S2 p.5).

In histological sections of acontia, the densely packed isorhizas and p-mastigophores were found cushioned by abundant large mucocytes at the base and in between cnidae (Fig. 8E–F). Two dense rows of nuclei were observed lateral to the base mid-line on the concave side of the filament. In longitudinally cut sections, the cnidocysts were oriented with their apex pointing at the margin of the convex side (Fig. 8E). Isorhizas could be identified by their light pink-stained tubule coils, making slightly oblique, transverse loops. The p-mastigophores were patchily distributed in between the isorhizas and stained a darker pink than the isorhiza tubules. Sometimes with the shaft recognizable as a fusiform shape surrounded by a pink haze of tubule, but mostly seen as a more diffuse strand (Fig. 8E). The capsule walls of cnidae were not visible in histological sections.

In cross-sectioned acontia, the isorhiza tubules were visible as bright pink circles, while the p-mastigophore tubules appeared as darker pink circles with a central dot (i.e. the shaft), or star-shaped, depending on where along the capsule and shaft they were sectioned (Fig. 8F). Mucocytes seemed to be confined to the margins and base, not in the central part of the acontia. The basal gastrodermis layer barely existed and was largely filled with mucocytes and a few pink blotches, possibly cnidoblasts.

Cnidome

1. *Microbasic b-mastigophores.* These could roughly be split into two normally distributed major size classes: small (12–23 μm) and large (30–48 μm), with a few intermediate (24–29 μm) in between. The distribution over tissues differed between size classes (Table 3, Fig. 2A). Small b-mastigophores were restricted to the gastrodermis, that is mesenterial filaments and acontia. In intact acontia, they were observed in the tissues in among the large cnidocysts. Large b-mastigophores were restricted to the epidermis, common throughout the tentacles, and found sparingly in the actinopharynx. The intermediate sized b-mastigophores were mainly in the actinopharynx, although a few were found in the mesenterial filaments and acontia.
   The capsule of the b-mastigophores was narrow and elongated, with parallel sides or slightly tapering towards the basal end, that is broadest in the apical region along the shaft (Figs 6C, 9E–G).
   The inverted shaft was thread-like, sometimes undulating, and varied in length, reaching 0.3–0.6 of the capsule length. The tubule usually filled the capsule and made dense regular coils around the shaft, creating a characteristic pattern, and more irregularly coiled basal to the shaft.
   The discharged shaft was microbasic, that is shorter than the capsule (Fig. 9R–S). The homotrichous shaft armature showed 3 or 5 coils of 1–2 μm long spines in triple helices for the respective size class. The transition between everted shaft and distal tubule was indistinct.
   The everted tubule was armed throughout with triple helices of tiny spines. The full length of a tubule of one small (capsule 15 μm) b-mastigophore was measured to c. 300 μm, while the tubule of a large capsule (41 μm) had a total length of c. 1000 μm.
2. *Microbasic and mesobasic p-mastigophores.* In all, the p-mastigophores could be divided into four size classes: small 13–22 μm, medium 23–34 μm, large 35–69 μm and very large 70–138 μm (Tables 2, 3, Figs 2B, 9B–C, H–I). The

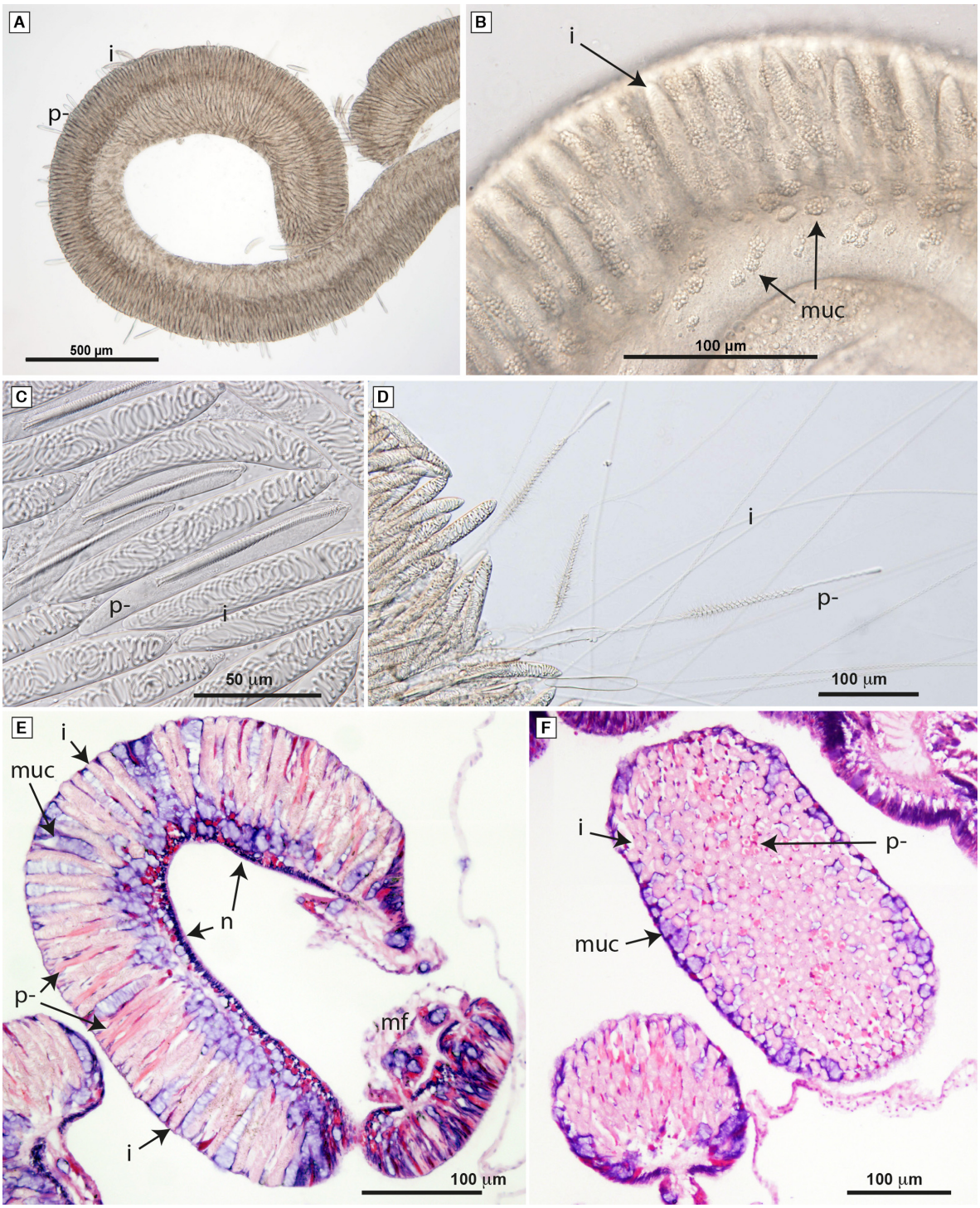

Fig. 8—Acontia. – A. Free coil of acontium packed with isorhizas (i) and p-mastigophores (p-). – B. Close-up of acontium with mucocytes (muc) interspersed among cnidae. – C. Densely packed cnidae: isorhizas (i) with capsules completely filled with irregular coils of tubule; p-mastigophores (p-) with shaft, and tubule coiled up in basal capsule. – D. Fired cnidae at the rim of an acontium: everted p-mastigophores (p-) with spined shafts, and holotrichous tubules of isorhizas (i). – E–F. Histological acontia preparations. – E. Longitudinally cut with pale pink isorhizas (i) with visible tubule coils and p-mastigophores (p-) as darker pink strands. Cnidae are cushioned by blue-stained mucocytes (muc). Dense rows of nuclei (n) seen at concave side (referred to as base midline in text) of acontium. – F. In cross-sectioned acontia the isorhiza (i) tubules are seen as bright pink circles, while p-mastigophore (p-) tubules are visible as circles with a central dot (shaft).

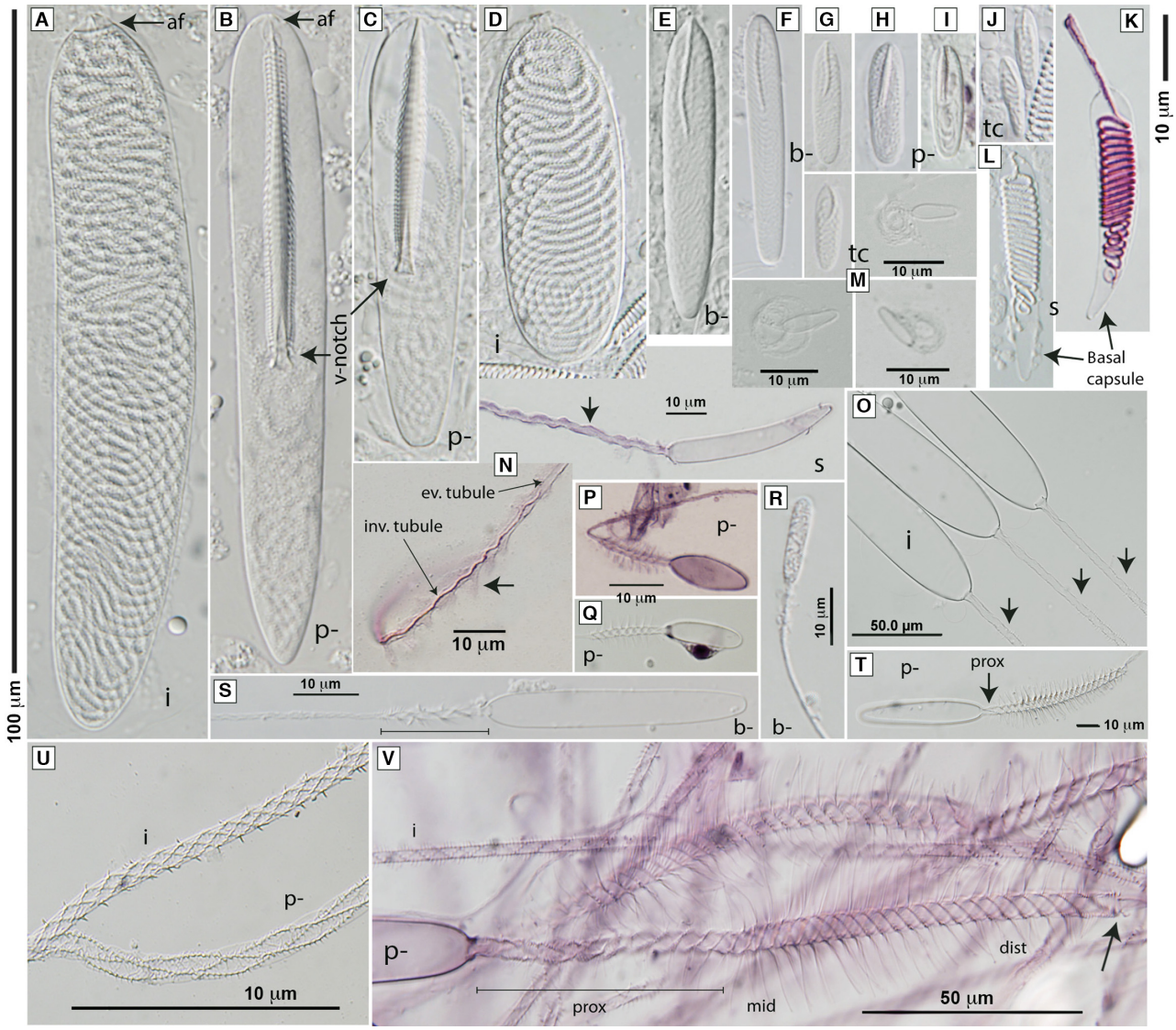

Fig. 9—Cnidome of *Lophelia pertusa*. – A-L and upper left M: intact capsules, all oriented with their apical ends up and basal ends down and in scale with the lateral scale bars. – M-V. Fired cnidae. – A. Very large acontia isorhiza (i) with visible apical flaps (af). Note pattern on tubule. – B. Very large acontia p-mastigophore (p-) with its sharp point (rod) of the shaft towards the apical flaps. – C. Large p-mastigophore (p-) from tentacles and mesenterial filaments. – D. Short, broad isorhiza (i) from tentacles. – E-G. b-mastigophores (b-) with typical thread-like shafts. – H-I. Small p-mastigophores (p-); present in all tissues, most abundant in column (v-notch vaguely visible). – J and upper left M: tiny cnidae (tc) of isorhiza-type. –K-L. Spirocysts (s), most abundant in tentacles; in K stained with eosin. – M. Everted tiny cnidae (tc) with coiled tubules. – N. Upper image: empty capsule of spirocyst (s) and everted tubule with single helix of eosinophilic microfibrillae still attached to tubule. Lower image: distal end of everted (ev.) tubule with microfibrillae adhering to glass slide. Note that the tubule is not fully everted; inverted (inv.) part is still inside. – O. Isorhiza (i) capsules with everted tubules showing variation in length of proximal spineless part (arrows point out first spine rows). – P-Q. Everted small p-mastigophore (p-) stained with nigrosin and eosin (note nucleus in Q). – R. Small b-mastigophore (b-) from mesenterial filaments and acontia. – S. Large b-mastigophore (b-) from tentacles and oral disk. – T. Medium p-mastigophore (p-) from mesenterial filaments; note short proximal (prox) part. – U. Everted tubules of isorhiza (i) and p-mastigophore (p-). – V. Stained everted very large p-mastigophore (p-). Shaft with long proximal part (prox), mid-part (mid) with long spines, distal part (dist) with successively shorter spines, and transition between shaft and tubule (arrow). Isorhiza (i) tubule also visible [Colour figure can be viewed at wileyonlinelibrary.com].

small were present in all tissues, albeit most abundant in tentacles and column. In actinopharynx and column, they were the only size class represented. The medium and large size classes were present in tentacles, mesenterial filaments and acontia, approximately equally common in the mesenterial filaments, while the large size class dominated

in the tentacles. The very large p-mastigophores were specific for the acontia and were there the second most abundant cnidocyst type after the large narrow isorhizas (Tables 2, 3). The p-mastigophores of the acontia were approximately twice the size compared to the large p-mastigophores in the tentacles and mesenterial filaments.

The capsule shape was highly variable in p-mastigophores of the mesenterial filaments, from rounded oval (prolate spheroids) to diamond shaped (Fig. 7D). The latter capsules were broadest alongside the v-notch of the shaft, and narrower at the apical and basal ends. The capsules of the small p-mastigophores were usually broad and symmetrically rounded oval, while capsules of the large ones were broader at the apical ends and slightly tapering towards the basal ends. The very large acontia p-mastigophores were narrow with almost parallel sides, sometimes slightly bent, and often tapering towards the basal ends that were either blunt or pointed.

The inverted shaft of the large and very large p-mastigophores was highly elaborate with its sharp point (rod) directed to the sometimes visible flaps at the apical end of the capsule (capsule aperture), and a conspicuous v-notch at the distal end of the shaft (Fig. 9B–C). The shaft reached half, or more than half (0.5–0.7), of the capsule length in the very large p-mastigophores (S1 p.5), and 0.4–0.6 of the capsule length in the small (S1 p.4). The shaft could be divided into three regions: the narrow proximal region towards the apical flaps, the broad mid-region and the distal part with the v-notch. In very large p-mastigophores (Fig. 9B), the narrow proximal end was longer than in the large p-mastigophores. The helical pattern on the twisted shaft was broader in the mid-region (Fig. 9B-C, S2 p.9), corresponding with the length of spines on the everted shaft, which were shorter at the proximal and distal ends and longest in the mid-region (Fig. 9V). The distal shaft region had a large, prominent v-shaped notch at its end (Fig. 9B–C). The v-notch depth varied between 1.5 μm in the small p-mastigophores and 11.5 μm in the largest. The cusps of the v-notch were sometimes bent and gave the notch the appearance of the forceps (i.e. cerci) of a male earwig (insect of the order Dermaptera).

The everted shaft was heterotrichous. The shaft of the very large p-mastigophores (158.4 ± 18.8 μm) was mesobasic (>1.5× the capsule length) and had 28 or 38 spine rows along the shaft (Fig. 9V). The proximal shaft was long and loose, and had approximately 1 spine row 10 μm^{-1}, armed with tiny (1–5 μm) spines. The mid-region was more regular, with 3 spine rows 10 μm^{-1} and armed with 10–13 μm long spines, which gradually grew shorter towards the distal end (Fig. 9V).

Small to large p-mastigophores were microbasic, with the everted shafts approximately as long, or shorter than, the capsule (Fig. 9P–Q, T). In large p-mastigophores (capsule c. 50 μm), the shaft had a short proximal part, and a mid-part with up to 6 μm long spines, and 18 or 20 spine rows on the entire shaft. The everted shafts of medium and small p-mastigophores had 12 or 15, and 5 or 7 spine rows, respectively. Roughly, the shaft doubled its length during eversion (S2 p.12).

The inverted tubule made a few irregular coils around the inverted shaft. Loose, irregular coils basal to the shaft nearly filled the remaining capsule of medium, large and very large p-mastigophores (Fig. 9B–C). In small p-mastigophores, the tubule seemed to fill the entire capsule (Fig. 9H).

The everted tubules were armed throughout with 1–2 μm long spines forming three helically arranged spine rows. Small p-mastigophores had 300–400 μm long tubules. The tubules of very large p-mastigophores were c. 4000 μm long and c. 4.1 μm broad, with 0.4–0.6 rows 10 μm^{-1}. The spine rows were widely spaced compared to the more regular rows of the isorhizas, and their everted tubules were thereby easily distinguished (Fig. 9U). The tubule of medium p-mastigophores was c. 1.5 μm broad. The full length of medium and large p-mastigophore tubules is unknown.

3. *Isorhizas* were present in tentacles and acontia with distinct populations in each tissue type. Broad oval isorhizas were sparsely scattered throughout the tentacles (54.4 ± 4.9 μm long, 18.3 ± 2.0 μm wide, length-to-width ratio 3 : 1, Fig. 9D). The large narrow isorhizas of the acontia were approximately twice as long (97.2 ± 12.6 μm long, 17.0 ± 1.6 μm wide, length-to-width ratio 6 : 1, Fig. 9A).

   The capsules of tentacle isorhizas were stout, symmetrically rounded oval (prolate spheroids), while acontia isorhizas were long and narrow, tapering to the basal end and often bent (Fig. 9A). The apical flaps were generally visible, sometimes with a protruding tip (Fig. 4F).

   The inverted tubule of the isorhizas made regular to irregular, slightly oblique coils, which mostly filled the entire capsule; however, a few isorhizas where observed in which the tubule did not fill the capsule.

   The everted tubule was holotrichous and reached up to 5000 μm in its full length. Proximally, the tubule was 2.6–3.8 μm broad, tapering slightly towards its end. It was armed throughout with uniform thorn-like spines (Fig. 9U) in very regular spine rows (1.8–2.2 spine rows 10 μm^{-1}), except for on the short proximal region close to the capsule that was more loose and free of spines. This proximal region varied in length (Fig. 9O).
4. *Tiny cnidae* (6–11 μm) were found sparingly in column and tentacles, and rarely in mesenterial filaments and acontia (Fig. 9J, M). Non-everted capsules appeared to have a shaft, although it could simply be a loop of the proximal tubule. When everted ones were found, they had a bent or spiraled and spined tubule, but no visible shaft. These tiny cnidae were most likely of isorhiza type.
5. *Spirocysts* were overwhelmingly numerous in the tentacles, extending down to the oral disc (Tables 2, 3, Figs 4, 5,

9K–L). A few spirocysts were found in other tissues but could not be confirmed in histological sections, therefore assumed to be cross-tissue contamination. The size distribution of the spirocysts was left-skewed and unimodal, with no discernible size classes (23.5 ± 5.7 μm, mean ± SD; mode 20.4 μm; range 12–42 μm, Fig. 2E–F).

The capsule shape varied from narrow, almost needle shaped, to broad. The length-to-width ratio varied between 3 : 1 and 10 : 1 with no indication of discrete types, that is capsule length-to-width ratios were normally distributed (S1 p.9). The capsules were broadest apically and tapered towards the narrow basal end (Fig. 9K–L).

The inverted tubule formed 20–30 distinct regular coils, transverse or slightly oblique, to the capsule axis and filled the capsule except for the narrow basal part. The first tubule coil in the apical part of the capsule was often seen as a loop perpendicular to the rest of the coils. The empty basal capsule part varied in length.

The everted tubule was broad, with a single helix of eosinophilic substance, probably microfibrillae or some component of these, winding along the entire tubule (Fig. 9N, upper). The microfibrillae sometimes spread out, giving a feathery appearance, and adhering to the glass slide surface (Fig. 9N, lower). The tips of semi-discharged tubules were sometimes capped, presumably by a droplet of agglutinant liquid (Fig. 4D).

Developing stages – cnidoblasts

Early stages of developing cnidocysts were either found in spherical cnidoblasts (Fig. 10A–B), or if the cnidoblasts were lysed, with the capsule and external tubule spread out (Fig. 10C). In fresh squash preparations, abundant developmental stages were present often in discrete regions sparse in mature cnidocysts (proliferation zones), although sometimes also interspersed among mature ones (Fig. 11A–B). As seen in histological sections, the cnidoblasts could be found mainly in the basal epidermis. In the tentacles, where the basal zones were wide the cnidoblasts were observed close to the mesoglea, completely separated from mature cnidae (Fig. 5A, C). In acontia and mesenterial filaments where the basal epidermis zones were narrower or almost absent, the cnidoblasts were found more interspersed among the bases of mature cnidae. The developing stages of isorhizas, p- and b-mastigophores (i.e. nematoblasts) seemed to develop in a very similar pattern (Fig. 10A–O), while spirocysts had a unique morphology during development (Fig. 11A–R).

Nematoblasts. Early nematoblasts had capsules with smooth external tubules (Fig. 10A–C). The developing p-mastigophores had heterogeneous tubule diameter; that is, the shaft region of the external tubule was wider than the tubule (Fig. 10A–B). Isorhizas could be identified by their larger capsule and homogeneous diameter of the external tubule (Fig. 10C).

In later stage nematoblasts with internalized tubules, isorhizas could be identified by their broad capsule, a tubule filling the entire capsule, and sometimes with a small protruding tip at the apical capsule end. The proximal part of the inverted tubule seemed to condense first, making the pattern of the tubule visible, while the remaining tubule was still obscure (Fig. 10D). The shafts of the b- and p-mastigophores were conspicuous, with the undulating thread-like shafts of b-mastigophores (Fig. 10M–N), and shafts with a v-notch of the p-mastigophores (Fig. 10E–L).

The shafts of p-mastigophores, however, seemed to invaginate primarily into an immature, slender and flexible shaft (Fig. 10E–F). A v-notch was present, but small. In addition, the immature capsules were more opaque than later stages, shafts and tubules diffused by capsule contents (Fig. 10D–H, M, S2 p.6). The shaft later untwined, that is relaxed its spiral twist around its axis, to allow for spines to develop (Fig. 10I–J). Spine helices were conspicuous in the loosened shafts, and the shaft could then reach the basal end of the capsule (Fig. 10I–J, S2 p.7). At this stage, the capsules became clear, with details of shaft and tubule distinct. When spines had been assembled, the spine helices were twisted and tightly tucked in along the shaft, sometimes displaying a double v-notch in the process (Fig. 10K).

Some shafts in immature capsules appeared fully developed, with a broader mid-region and a deep v-notch (Fig. 10G–H), although the opacity of the capsule did not allow any details to be discerned. Further, it seemed as if most of the still bent p-mastigophores were in an immature stage (Fig. 10E–G), although a few capsules were still bent at later stages (Fig. 10L). In a mature shaft, the spines are seen as

Fig. 10—Developing stages of nematocysts. – A-B. Intact cnidoblasts (p-mastigophores) with capsules and heterogeneous diameter of external (ext.) shaft and tubule. – C. Isorhiza with broad large capsule, and homogenous tubule diameter (cnidoblast has lysed). – D. Isorhiza at later stage of development; tubule internalized and with its proximal part condensed, spines developing. A protruding (prot.) tip at the apical end. – E–L. Different stages of p-mastigophore development; internalized tubule and recognizable shaft with v-notch. – E–F. Shafts slender and immature, before spines are formed. Cnidoblast (cb) intact in E. – F. Capsule is starting to unfold. – G–H. Still present cnidoblast, capsule unfolding. – I-J. Final maturation: the shaft is untwined to make room for spine development, spine helices (sh) projecting, the v-notch sometimes reaching basal end of capsule. – K–L. The shaft is re-packed, getting shorter as it is twisted tighter, and spine helices (sh) are less projecting. – M–O. Developing b-mastigophores with typical thread-like, sometimes undulating shafts. – M. Shaft visible, tubule is diffuse. – N. The tubule has condensed and is seen filling up the entire capsule. – O. Shaft untwined, almost reaching the basal end. Note the even diameter of the proximal shaft at its point of attachment to the apical capsule end, unlike the pointed shaft of p-mastigophores. *All scale bars 10 μm [Colour figure can be viewed at wileyonlinelibrary.com].

indentations along the sides of the shaft, although, when focus is placed on top of the shaft, the tightly packed spine helices can be seen as transverse bands (Fig. 9B–C, S2 p.9).

Developing b-mastigophores displayed a similar stage with an untwined shaft reaching the basal end of the capsule (Fig. 10O). Very few b-mastigophore cnidoblasts were

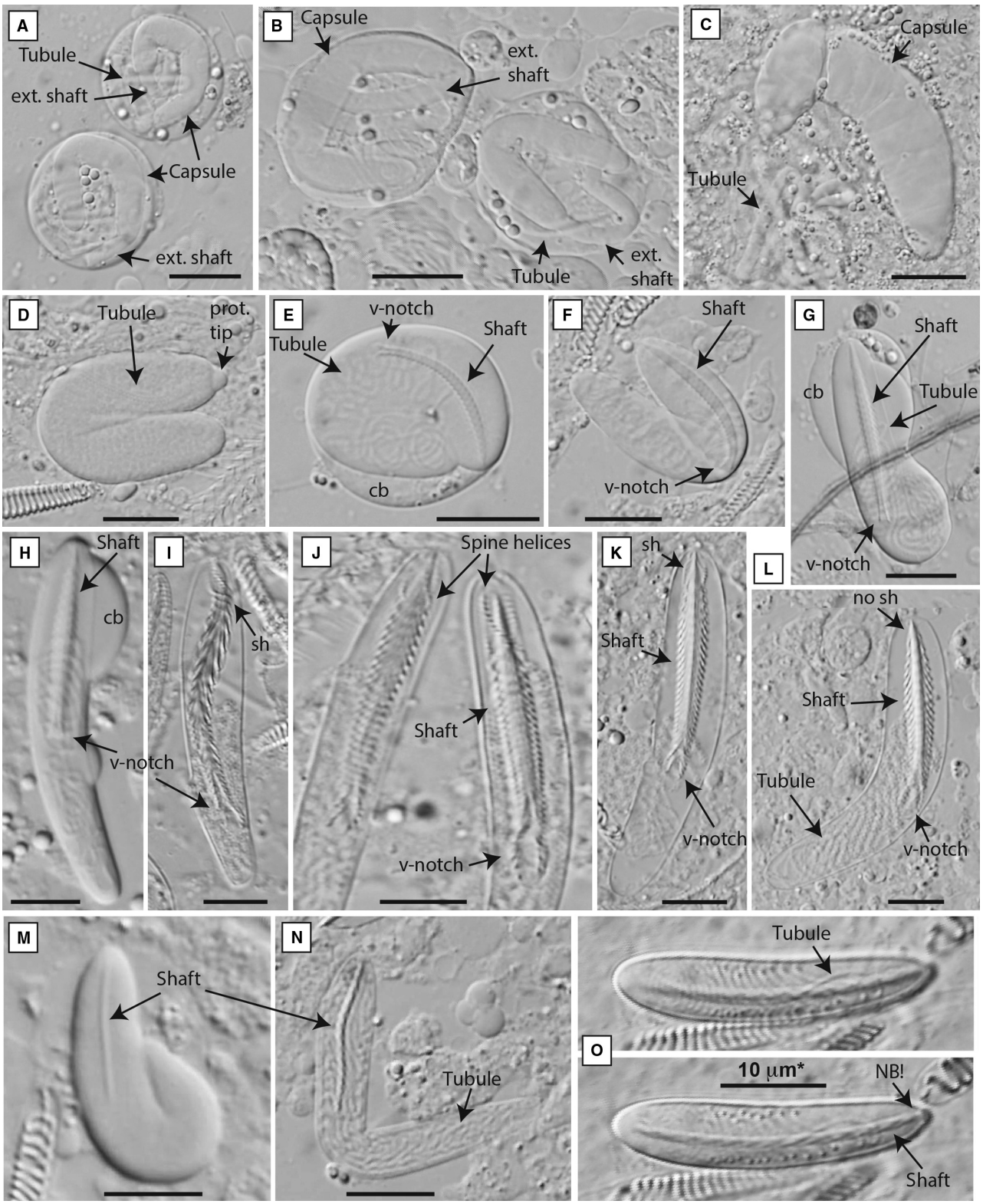

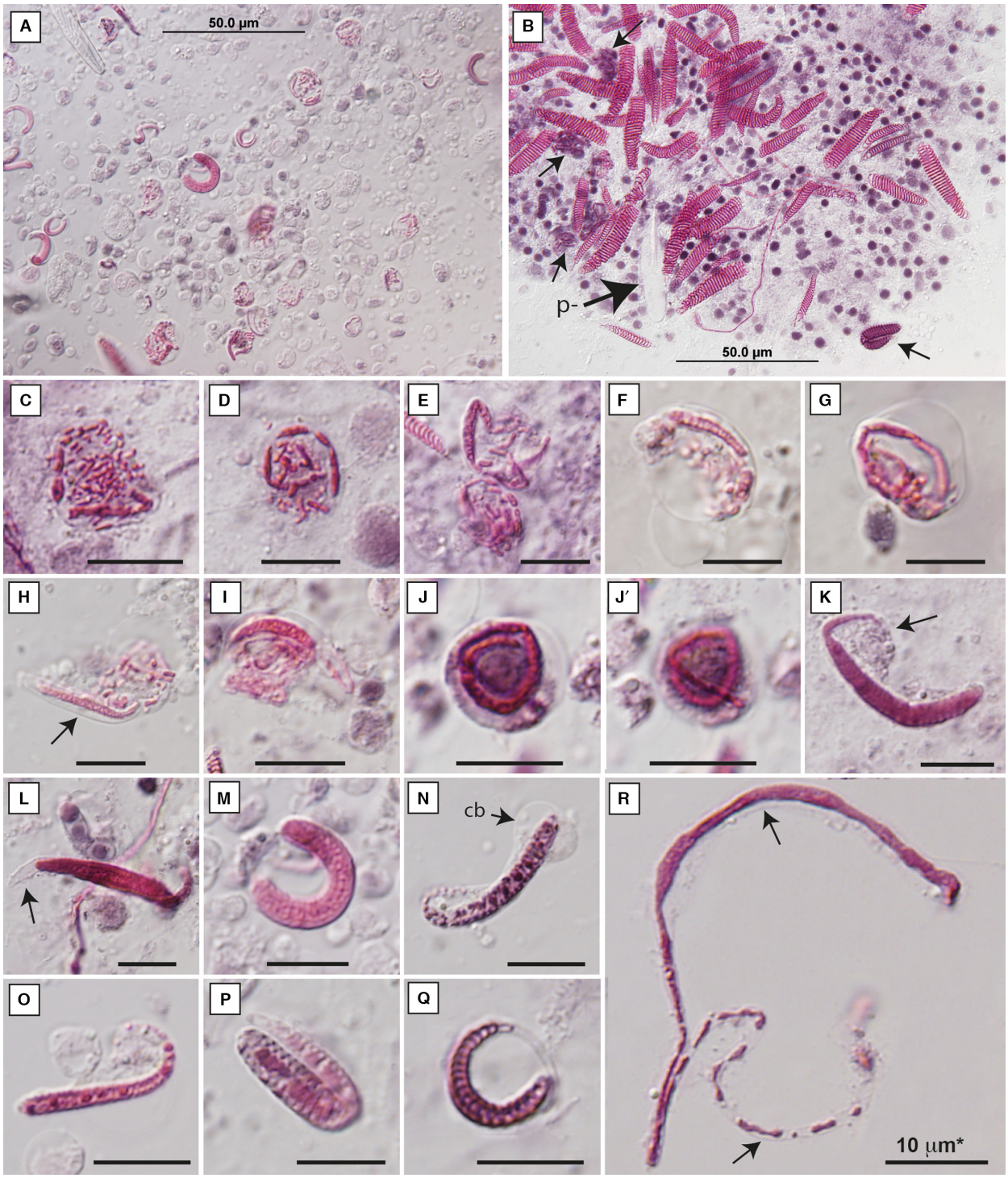

Fig. 11—Developing stages of spirocysts. – A. Area dominated by developing stages. – B. Cnidoblasts (small arrows) among mature spirocysts. The p-mastigophores (p-) not stained. – C–E. Early stages of developing spirocysts. The eosinophilic substance inside the external tubule is excreted in fragments. – F–I. Tubule with eosinophilic substance is packed into the capsule. Arrow in H point out capsule. – J–J′. Intact spiroblast (the same taken in two different focus planes). – K–L. Lysed cnidoblasts: the external tubule is almost completely internalized into the capsules (arrow in K point out external tubule). – L. Empty basal capsule end (arrow). –M. The entire tubule internalized. – N–P. Late stage spiroblasts where the eosinophilic substance seems to rearrange. – Q. Maturing spirocyst: the coils are discernable. – R. A lysed spiroblast has released an external tubule with its eosinophilic content, making the tubule walls visible (arrows). *Scale bars in C-R 10 µm.

observed, and the details of the stages of development cannot be resolved here. The untwined shaft had a homogeneous diameter, with no visible pointed rod towards the apical end as in p-mastigophores.

Spiroblasts. Developing spirocysts was easily identified in stained preparations. The tubule was filled with eosinophilic substance, initially built up by short fragments (Fig. 11C–F). In a lysed spiroblast, with its external tubule spread out on the glass slide, the eosinophilic substance clearly was contained within a thin-walled tubule (Fig. 10R). In non-stained preparations, using Normarski light microscopy, the spiroblast tubule seemed to be completely fragmented because the tubule itself was not visible (S2 p.8). The fragments were subsequently merging and packed into the capsule (Fig. 11F–I). In some spiroblasts, it seemed as if an outer tubule were left outside the capsule, that is not inverted along with the eosinophilic matrix and inner tubule (Fig. 11K). The eosinophilic substance was initially packed into the capsule as a seemingly undifferentiated mass (Fig. 11J–L), that later rearranged and condensed until the tubule coils were visible (Fig. 11M–Q). In everted tubules of fired spirocysts, the eosinophilic substance was found in a single helix along the tubule, or feathering out attaching to the glass slide (Fig. 9N), and is assumed to be the microfibrillae described by Mariscal *et al.* (1977b) or a component thereof.

Discussion

Comparison with the description of Carlgren

The cnidome of polyps of *Lophelia pertusa* (Linnaeus, 1758) from newly collected material was in close agreement with the cnidae descriptions of *Lophohelia prolifera* (Pallas, 1766) made by Carlgren (1940). Carlgren reported microbasic b-mastigophores, microbasic p-mastigophores, holotrichs (=holotrichous isorhizas) and spirocysts (Table 1). The size ranges of cnidae examined by Carlgren were within the size ranges in this study (Table 2). Carlgren did not provide data on the number of measurements taken, but one can assume that he measured fewer than in the present study, and the discrepancy is probably mostly due to chance, or possibly that he examined preserved material.

The smallest cnidae observed by Carlgren were 14 μm (b- and p-mastigophores from filaments and actinopharynx, Table 1). In our examinations, we have identified b-mastigophores down to 12 μm, p-mastigophores down to 13 μm and, in addition, a new tiny cnida of isorhiza type of 6–11 μm (Table 2).

The *microbasic b-mastigophores* reported by Carlgren (1940, pp. 44–45) were found sparsely in tentacles, actinopharynx and filaments. The inverted shaft of the tentacle b-mastigophores he described as very short, with 3 spine rows in the everted shaft armature (Carlgren 1940; p. 46. Fig. XV13–14). The size ranges of medium microbasic b-mastigophores in our material corresponded well to the size ranges of the microbasic b-mastigophores in Carlgren's material (see Tables 1, 2). The number of spine rows on everted shafts was usually 3, but 5 spine rows were found in the larger b-mastigophores. He found large b-mastigophores in the tentacles and small in the filaments, and the same pattern of distribution was found in our study. Although Carlgren defined b-mastigophores as sparse in all tissues, they were found to be common (tentacles, acontia), or numerous (mesenterial filaments) in the present material.

Microbasic p-mastigophores, Carlgren (1940, pp. 44–46) divided into three size classes. Small p-mastigophores he reported from column, tentacles and actinopharynx, congruent with the present study. The largest p-mastigophores Carlgren reported 'only in the lower, strongly coiled parts of the filaments': interpreted as the acontia and correlating with the very large p-mastigophores in our study. The intermediate size class Carlgren reported from tentacles and filaments are corresponding to our medium and large size classes (from tentacles and mesenterial filaments). While Carlgren observed 10 spine rows in the everted shafts of the tentacle p-mastigophores, and 15 spine rows in the largest p-mastigophores (Carlgren 1940; pp. 45, 46, Fig. XV17), the corresponding p-mastigophores in our study showed 15 or 18, and 28 or 38 spine rows, respectively (Tables 1, 2). Most probably, Carlgren did not observe the small spines on the proximal and distal shaft regions and had thus only counted the spine rows from the mid-shaft region with the most conspicuous spines. Carlgren reported the larger p-mastigophore shafts as being 'somewhat longer than the capsule'. In our material, it was clear that they were more than 1.5 times longer than the capsule, and therefore, we here re-classify them as mesobasic according to the nomenclature of Östman (2000). Carlgren made a note on the smaller p-mastigophores in the filaments that they were 'possibly not hoplotelic' (i.e. spined on both shaft and tubule), but in the present material spines were present along the full length of the everted tubules.

Holotrichs were sparingly distributed in tentacles and actinopharynx, and dense in acontia (i.e. 'the strongly coiled part of filaments'), according to Carlgren. The large holotrichs observed by Carlgren correspond to our large and narrow holotrichous isorhizas from the acontia, and the sizes of holotrichs in tentacles and actinopharynx correspond to the broad oval isorhizas. The holotrichs he found in the actinopharynx could be contamination from the tentacles, but it is also possible that they extend to the oral disc although we did not find any. The difficulties of reliably dissecting out tissue from the actinopharynx left us with very few samples of that specific tissue type.

Spirocysts, Carlgren found to be very numerous in the tentacles, rare in the filaments, and not present in the actinopharynx. As spirocysts were so conspicuous in eosin-stained preparations, we are confident that they are not present in mesenterial filaments or acontia because they were absent in stained histological preparations of those tissues. Contrary to

the mesenterial filaments, spirocysts are confirmed on the oral disc close to the actinopharynx.

Comparison between fresh and histological preparations

Comparing preparations of live tissues with haematoxylin and eosin-stained histological sections of the same tissues was useful to verify the presence or non-presence of cnidocysts and secretory cells, and their organization within tissues. In some cases, the comparisons could be of help in identifying cross-tissue contaminations of cnidae, as mentioned above. This was especially useful considering spirocysts that were highly eosinophilic and easily identified. If they were present, they could not be missed in stained tissues. The nematocysts, however, were less well visualized. The poor fixation and staining of nematocysts in the histological preparations is probably due to improper methods. The capsules are soluble in alkaline reducing agents, especially disulphide reducing agents (Blanquet and Lenhoff 1966; David *et al.* 2008). The collapsing of capsules made it more difficult to recognize nematocysts in the tissues. The shaft and tubules of the nematocysts were also eosinophilic, although much less so than the tubule content of spirocysts. It was therefore less useful to use histological slides to confirm presence of nematocysts in tissues, especially in the mesenterial filaments and oral gastrodermis that were intensely stained by basophilic components.

Developing cnidae

The different *developing stages* observed in this study are to a large extent congruent with previous descriptions of cnidogenesis (Slautterback and Fawcett 1959; Westfall 1966; Skaer 1973; Holstein 1981; Tardent and Holstein 1982; Östman *et al.* 2010a,b, 2013). The location of cnidoblasts mainly in the basal epidermis below mature cnidae is in agreement with Möbius (1866) and Slautterback and Fawcett (1959), although cnidoblasts were also found among mature cnidae. Dense populations of cnidoblasts in discrete proliferation zones, with few or no mature cnidae were also observed (Fig. 11A), as previously noted in the sea anemones *Metridium senile* and *Sagartiogeton viduatus* (Östman *et al.* 2010a,b, 2013).

The novelty of cnidogenesis observed in this study concerns the p-mastigophore shaft and its v-notch. It has been stated that spines differentiate immediately after invagination of the external tubule (Holstein 1981). In this study, we have observed a time lag, with untwining of the shaft (relaxation of the spiral twist around its axis) between invagination and spine assembly; before the final packaging of the mature shaft in which the shaft again is tightly twisted around its axis. The p-mastigophore shafts thus undergo invagination, in which they are twisted and pleated into a recognizable, but immature, shaft with a v-notch. Immature shafts have a less pronounced increase of the diameter of the mid-region, appearing more slender, and a small v-notch. Later, the shaft untwines to allow for spine development. When this is completed, the shaft undergoes a second packaging, twisted and pleated into the mature, spined shaft, now with a larger v-notch. The small v-notch in the immature shaft is due to the difference in diameter between shaft region and tubule, and when spines are added, this difference increases.

In *Hydra*, spine development has been thoroughly mapped, and a glycine- and histidine-rich protein named spinalin identified as the major component (Koch *et al.* 1998). Spines develop in the lumen of the inverted tubule and shaft, with the electron-dense precursors first present in the matrix of the capsule before invagination of the external tubule (Holstein 1981; Koch *et al.* 1998; Hellstern *et al.* 2006). This protein has not yet been identified in anthozoans; however, it is likely the same (or a similar) protein responsible for spine assembly within Anthozoa. The opacity of the immature capsules seen in Fig. 10E–H could thus be due to the precursors of spines, that is electron-dense subunits. Once the spines have assembled, the subunits are used-up and the capsule is clear (Figs 9B–C, 10I–L). The shafts in Fig. 10G–H that appear to be mature, with broader mid-diameter and larger v-notch, could possibly be due to the shaft beginning to loosen up and untwine before spine development. The opacity of the capsule suggests that spine assembly has not yet taken place.

Early stages of developing cnidae of different types are difficult to discern from one another at the very earliest stages of development, although there are some early indicators of the complexity of the end product. It appears that the extension of the endoplasmic reticulum (Slautterback and Fawcett 1959) and the number of microtubuli formed by the centrioles (forming the cage around the growing tip of the external tubule) is related to the size and complexity of the capsule and shaft region under construction (Holstein 1981). This is however only visible in TEM sections. In light microscopy, it is sometimes possible to see that the external tubule has a heterogeneous diameter, that is the shaft region is wider than the tubule. This could be observed in some of the nematoblasts (Fig. 10A-B), and was described also by Holstein (1981). As p-mastigophores have a more elaborate shaft than b-mastigophores, with larger difference in diameter between shaft and tubule, it should be possible to discern the two types, although during this study we did not find any distinct examples. The nematoblasts of isorhizas were more readily discerned from the other nematocyst types, due to their lack of shaft and therefore homogenous diameter of the external tubule, and the large size of the capsule. The spiroblasts were the easiest ones to discern from the others, especially in stained preparations, due to their highly eosinophilic substance.

Most efforts in describing cnidocyst development have been devoted to nematocysts, while spirocyst development has been addressed only by Kupson and Greenwood (1989), published as an abstract in *American Zoologist*. The

fundamentals of spirocyst development seem to be the same as for nematocysts; however, the morphological differences, such as the thin tubule wall and the eosinophilic substance, can produce artefacts using light microscopy. The apparent fragmentation of the tubule as seen in unstained Normarski micrographs (S2 p.8) is due to the thin tubule wall and fragmented eosinophilic substance. When the material was stained with eosin and documented in fresh preparations, the tubule wall was visible, and it was obvious that only the eosinophilic substance was fragmented. The single helix of microfibrillae, in contrast to the triple helices of spines on nematocysts, is another unique characteristic of spirocysts. This is congruent with previous descriptions of spirocyst tubules (Schmidt 1969; Mariscal *et al.* 1977b).

The lack of attention given to spiroblasts in previous literature prompted us to devote more effort into their development. The abundance of developing stages varies over time, and between polyps, depending on a recent event of large-scale discharge. One dissected polyp was especially rich in spiroblasts in the tentacles, and almost all images of spiroblasts are from that one polyp. It is estimated that replenishing takes almost a week (Schmidt 1982), and thus, cnidoblasts could be experimentally induced by poking or air exposure of tentacles to stimulate large-scale discharge. Cnidoblasts should be present within the next few days. This probably occurred in the dissected polyp rich in spiroblasts, although not planned.

A remark on the function of cnidae

The distribution of different cnidae types and size classes in different tissues probably reflect their function. Coral polyps are delicate, and feeding involves high risk when handling prey such as copepods with exoskeletons and sharp appendages. The agglutinant spirocysts and entangling isorhizas in the tentacles are perfect adaptations, efficiently immobilizing the prey until the toxins delivered by the penetrating large b- and p-mastigophores take effect.

The largest cnidae in the acontia has been attributed to a function mainly in aggression (Kramer and Francis 2004; Nevalainen *et al.* 2004). As a predator or aggressor approaches the polyp, the acontia are extruded through the mouth as the polyp quickly retracts, and the very large cnidae can fire. These very large cnidae are also found in the mucus strands released by *L. pertusa* when they have been handled, after quick polyp retraction when touched (personal observation). The dominance of penetrating cnidae in the mesenterial filaments could be due to the nature of the toxins, which contain enzymes and thus aid in digestion of the captured prey (Nevalainen *et al.* 2004). A study by Schlesinger *et al.* (2009) showed that the acontial microbasic p-mastigophores of the sea anemone *Aiptasia diaphena* penetrates prey inside the gastrovascular cavity when the animal is feeding. A function in feeding and digestion is thus also probable for the large acontia cnidae.

The tiny cnidae and abundant small p-mastigophores in the external tissue layer (column) on the theca could provide an explanation for the absence of epifauna on the surfaces of the skeleton covered with live tissue. Only, a few species are seen in direct contact with living branches of *Lophelia pertusa*, for example the crustacean *Munidopsis serricornis* and the polychaete *Eunice norvegica* (usually protected within its tube), while dead coral branches house a myriad of fouling invertebrates. The cnidae of the column could thus be an efficient antifouling agent.

A final remark on the use of the term acontia

The authors are aware that the term *acontia* has not previously been used to distinguish the free coils of the mesenterial filaments in scleractinians. However, the descriptions of acontia from sea anemones fit well with the structures observed in *Lophelia pertusa*.

Carlgren (1949) describes acontia as: 'thin threads attached at one end to mesenteries, as a rule below the filaments, while the other end is free. They are laden with extraordinarily numerous nematocysts of variable categories'. Gosse (1860, p. XXV of the Introduction) provided more detail in the morphology by describing the point of insertion to be anywhere along the cnidoglandular band (named 'craspeda' by Gosse) of the mesenteries, rather than 'below the filaments' as Carlgren (1949) stated. Stephenson (1920, pp. 443–445) provided the most detailed description of acontia. He made a comparison between acontia and mesenterial filaments, and distinguished one from the other, simultaneously stating: 'an acontium can only be regarded as a specialized form of mesenterial filament'. In addition, Stephenson (1920) suggested that acontia 'help to paralyse prey and to defend the animal'. He further warned that acontia of some species can be 'partially reduced or even quite rudimentary'. An example of rudimentary acontia is the nematosomes of *Nematostella vectensis,* that is small globular bodies containing cnidocysts, rotating freely in the gastrovascular cavity. These were suggested by Williams (1979) to be homologous to acontia and acontoids (thicker filaments with less cnidae, Carlgren 1949), because they bud off from the cnidoglandular bands.

The descriptions fit well with the morphology of the structures we have chosen to call acontia in *L. pertusa:* that is, firstly, they emanate from the cnidoglandular band; secondly, they are structurally distinct from the mesenterial filaments, both in morphology and function, and in this aspect congruent with acontia. Generally, the cnidae of the acontia are larger than in the mesenterial filaments, although marginally so in some species (Stephenson 1920; Carlgren 1945). In *L. pertusa,* they are much larger than the cnidae in the mesenterial filament, similar to what is found in the sea anemone family Sagartiidae, described by Carlgren (1945).

Following that mesenteries and their filaments are a common character of the basic bauplan within Anthozoa (Daly

et al. 2003), and the acontia are specialized parts of the mesenterial filaments, then acontia might well be an ancestral condition within Anthozoa that has been lost multiple times. Rodríguez *et al.* (2012), for example, have found acontia to be lost, or reduced, several times within Actiniaria (sea anemones).

We suggest that a more thorough examination of acontia within scleractinians should be carried out to re-evaluate the status of acontia within Anthozoa as a whole. Other species of azooxanthellate, temperate or deep-sea scleractinians, which feed on larger prey such as copepods, might also have retained their acontia; for instance, we have observed similar structures in the temperate cup-coral *Caryophyllia smithii*.

Acknowledgements

The study was carried out at the Sven Lovén Center for Marine Sciences, Tjärnö, a marine field station belonging to the University of Gothenburg. Financial support was obtained from FORMAS (contract No. 2010-1604), and the faculty of Science of Uppsala University. We would like to express deep gratitude to the anonymous reviewer who provided us with many knowledgeable and useful comments that helped us improve this manuscript.

Supporting Information

Additional supporting information may be found in the online version of this article:

Data S1. Supplemental tables and graphs.

Data S2. Supplemental images.

References

Abramoff, M. D., Magalhaes, P. J. and Ram, S. J. 2004. Image processing with Image J. – *Biophotonics International* **11**: 36–42.

Blanquet, R. and Lenhoff, H. M. 1966. A disulfide-linked collagenous protein of nematocyst capsules. – *Science* **154**: 152-&.

Carlgren, O. 1940. A contribution to the knowledge of the structure and distribution of cnidae in the Anthozoa. – *Acta Universitatis Lundensis (ser 2)* **36**: 1–62.

Carlgren, O. 1945. Further contributions to the knowledge of the cnidom in the Anthozoa especially in the Actiniaria. – *Lunds Universitets Årsskrift* **41**: 1–24.

Carlgren, O. 1949. A survey of the Ptychodactiaria, Corallimorpharia and Actiniaria. – *Kungliga Svenska Vetenskapsakadamiens Handlingar* **1**: 1–121.

Colin, S. P. and Costello, J. H. 2007. Functional characteristics of nematocysts found on the scyphomedusa *Cyanea capillata*. – *Journal of Experimental Marine Biology and Ecology* **351**: 114–120.

Cutress, C. E. 1955. An interpretation of the structure and distribution of cnidae in Anthozoa. – *Systematic Zoology* **4**: 120–137.

Dahl, M. P., Pereyra, R. T., Lundälv, T. and André, C. 2012. Fine-scale spatial genetic structure and clonal distribution of the cold-water coral *Lophelia pertusa*. – *Coral Reefs* **31**: 1135–1148.

Daly, M., Fautin, D. G. and Cappola, V. A. 2003. Systematics of the Hexacorallia (Cnidaria: Anthozoa). – *Zoological Journal of the Linnean Society* **139**: 419–437.

David, C. N., Ozbek, S., Adamczyk, P., Meier, S., Pauly, B., Chapman, J., Hwang, J. S., Bojobori, T. and Holstein, T. W. 2008. Evolution of complex structures: Minicollagens shape the cnidarian nematocyst. – *Trends Genet* **24**: 431–438.

Dodds, L. A., Black, K. D., Orr, H. and Roberts, J. M. 2009. Lipid biomarkers reveal geographical differences in food supply to the cold-water coral *Lophelia pertusa* (Scleractinia). – *Marine Ecology-Progress Series* **397**: 113–124.

Fautin, D. G. 2009. Structural diversity, systematics, and evolution of cnidae. – *Toxicon* **54**: 1054–1064.

Fautin, D. G. 2013. Hexacorallians of the world. Sea anemones, Corals, and their allies. http://geoportal.kgs.ku.edu.edu/hexacorall/anemone2/index.cfm. Recent update of functionality: 2nd January 2013.

Fautin, D. G. and Mariscal, R. N. 1991. Cnidaria: Anthozoa. In: Harrison, F. W. and Westfall, J. A., (Eds): Microscopic anatomy of Invertebrates, vol. **2**, pp. 267–358. – Wiley-Liss, N.Y.

Freiwald, A., Fosså, J. H., Grehan, A., Koslow, T. and Roberts, M. J. 2004. Cold-water coral reefs: Out of sight – no longer out of mind. 83 pp. UNEP-WCMC, Cambridge, UK.

Gass, S. E. and Roberts, J. M. 2010. Growth and branching patterns of *Lophelia pertusa* (Scleractinia) from the North Sea. – *Journal of the Marine Biological Association of the United Kingdom* **91**: 831–835.

Gosse, P. H. 1860. Actinologia Britannica: A history of the British sea-anemones and corals, 362 pp. Van Voorst, Paternoster Row, London.

Hellstern, S., Stetefeld, J., Fauser, C., Lustig, A., Engel, J., Holstein, T.W. and Özbek, S. 2006. Structure/function analysis of spinalin, a spine protein of *Hydra* nematocysts. – *Federation of European Biochemical Societies Journal* **273**: 3230–3237.

Holstein, T. 1981. The morphogenesis of nematocytes in *Hydra* and *Forskålia*: An uItrastructural study. – *Journal of Ultrastructure Research* **75**: 276–290.

Kass-Simon, G. and Scappaticci, A. A. 2002. The behavioral and developmental physiology of nematocysts. – *Canadian Journal of Zoology-Revue Canadienne De Zoologie* **80**: 1772–1794.

Koch, A. W., Holstein, T. W., Mala, C., Kurz, E., Engel, J. and David, C. N. 1998. Spinalin, a new glycine- and histidine-rich protein in spines of Hydra nematocysts. – *Journal of Cell Science* **111**: 1545–1554.

Kramer, A. and Francis, L. 2004. Predation resistance and nematocyst scaling for *Metridium senile* and *M. farcimen*. – *The Biological Bulletin* **207**: 130–140.

Kupson, J. E. and Greenwood, P. G. 1989. Spirocyst development in the sea-anemone *Haliplanella luciae*. – *American Zoologist* **29**: A110–A110.

Larsson, A. I., Järnegren, J., Strömberg, S. M., Dahl, M. P., Lundälv, T. and Brooke, S. 2014. Embryogenesis and larval biology of the cold-water coral *Lophelia pertusa*. – *Plos One* **9**: e102222.

Mariscal, R. N. 1974. Scanning electron microscopy of the sensory surface of the tentacles of sea anemones and corals. – *Cell and Tissue Research* **147**: 149–156.

Mariscal, R. 1984. Cnidaria: Cnidae. In: Bereiter-Hahn, J., Matoltsy, A. G. and Richards, K. S., (Eds): Biology of the Integument, pp. 57–68. – Springer, Berlin Heidelberg.

Mariscal, R. N., Conklin, E. J. and Bigger, C. H. 1977a. The ptychocyst, a major new category of cnidae used in tube construction by a cerianthid anemone. – *The Biological Bulletin* **152**: 392–405.

Mariscal, R. N., McLean, R. B. and Hand, C. 1977b. The form and function of cnidarian spirocysts. 3. Ultrastructure of the thread and the function of spirocysts. – *Cell and Tissue Research* **178**: 427–433.

Möbius, K. A. 1866. Ueber den Bau, den mechanismus und die entwicklung der nesselkapseln einiger polypen und quallen.

– *Abhandlungen aus dem Gebiete der Naturwissenschaften Hamburg* **V**: 1–22, pls. 1–2.

Mueller, C. E., Larsson, A. I., Veuger, B., Middelburg, J. J. and van Oevelen, D. 2013. Opportunistic feeding on various organic food sources by the cold-water coral *Lophelia pertusa*. – *Biogeosciences Discussions* **10**: 11375–11403.

Nevalainen, T. J., Peuravuori, H. J., Quinn, R. J., Llewellyn, L. E., Benzie, J. A. H., Fenner, P. J. and Winkel, K. D. 2004. Phospholipase A2 in Cnidaria. – *Comparative Biochemistry and Physiology B-Biochemistry & Molecular Biology* **139**: 731–735.

Östman, C. 2000. A guideline to nematocyst nomenclature and classification, and some notes on the systematic value of nematocysts. – *Scientia Marina* **64**: 31–46.

Östman, C., Kultima, J. R. and Roat, C. 2010a. Tentacle cnidae of the sea anemone *Metridium senile* (Linnaeus, 1761) (Cnidaria: Anthozoa). – *Scientia Marina* **74**: 511–521.

Östman, C., Kultima, J. R., Roat, C. and Rundblom, K. 2010b. Acontia and mesentery nematocysts of the sea anemone *Metridium senile* (Linnaeus, 1761) (Cnidaria: Anthozoa). – *Scientia Marina* **74**: 483–497.

Östman, C., Borg, F., Roat, C., Roat Kultima, J. and Wong, S.Y.G. 2013. Cnidae in the sea anemone *Sagartiogeton viduatus* (Muller, 1776) (Cnidaria, Anthozoa); A comparison to cnidae in the sea anemone *Metridium senile* (Linnaeus, 1761) (Cnidaria, Anthozoa). – *Acta Zoologica* **94**: 392–409.

Robson, E. A. 2004. Cnidogenesis in the jewel anemone *Corynactis californica* (Carlgren, 1936) and *C. viridis* (Allman, 1846) (Anthozoa: Corallimorpharia). – *Zoologische Mededelingen (Leiden)* **78**: 461–476.

Rodríguez, E., Barbeitos, M., Daly, M., Gusmão, L. C. and Häussermann, V. 2012. Toward a natural classification: Phylogeny of acontiate sea anemones (Cnidaria, Anthozoa, Actiniaria). – *Cladistics* **28**: 375–392.

Schlesinger, A., Zlotkin, E., Kramarsky-Winter, E. and Loya, Y. 2009. Cnidarian internal stinging mechanism. – *Proceedings of the Royal Society of London B: Biological Sciences* **276**: 1063–1067.

Schmidt, H. 1969. Die Nesselkapseln der Aktinien und ihre differentialdiagnostische Bedeutung. – *Helgolander Wissenschaftliche Meeresuntersuchungen* **19**: 284–317.

Schmidt, G. H. 1982. Replacement of discharged cnidae in the tentacles of *Anemonia sulcata*. – *Journal of the Marine Biological Association of the United Kingdom* **62**: 685–691.

Skaer, R. J. 1973. The secretion and development of nematocysts in a siphonophore. – *Journal of Cell Science* **13**: 371–393.

Skaer, R. J. and Picken, L. E. R. 1966. The pleated surface of the undischarged thread of a nematocyst and its simulation by models. – *Journal of Experimental Biology* **45**: 173–177.

Slautterback, D. B. and Fawcett, D. W. 1959. The development of the cnidoblasts of *Hydra*: An electron microcope study of cell differentiation. – *Journal of Biophysical and Biochemical Cytology* **5**: 441–467.

Stephenson, T. A. 1920. Memoirs: On the Classification of Actiniaria. – Part I. – Forms with acontia and forms with a mesogloeal sphincter. – *Journal of Cell Science* **s2-64**: 425–572.

Tardent, P. 1995. The cnidarian cnidocyte, a high-tech cellular weaponry. – *Bioessays* **17**: 351–362.

Tardent, P. and Holstein, T. 1982. Morphology and morphodynamics of the stenotele nematocyst of *Hydra attenuata* Pall. (Hydrozoa, Cnidaria). – *Cell and Tissue Research* **224**: 269–290.

Weill, R. 1934. Contribution à l' étude des cnidaires et de leurs nématocystes. I, II. – *Travaux de la Station Zoologique de Wimereux* **10,11**: 1–701.

Westfall, J. A. 1966. Differentiation of nematocysts and associated structures in Cnidaria. – *Zeitschrift Fur Zellforschung Und Mikroskopische Anatomie* **75**: 381–403.

Williams, R. B. 1979. Studies on the nematosomes of *Nematostella vectensis* Stephenson (Coelenterata: Actiniaria). – *Journal of Natural History* **13**: 69–80.

Wilson, J. B. 1979. Patch development of the deep-water coral Lophelia pertusa (Linnaeus, 1758) on Rockall Bank. – *Journal of the Marine Biological Association of the United Kingdom* **59**: 165–177.

WoRMS Editorial Board. 2014. World Register of Marine Species. Available from http://www.marinespecies.org at VLIZ.

Yamashita, K., Kawaii, S., Nakai, M. and Fusetani, N. 2003. Larval behavioral, morphological changes, and nematocyte dynamics during settlement of actinulae of *Tubularia mesembryanthemum*, Allman 1871 (Hydrozoa: Tubulariidae). – *Biological Bulletin* **204**: 256–269.

